U.S. DEPARTMENT OF COMMERCE
NATIONAL OCEANIC AND ATMOSPHERIC ADMINISTRATION
NATIONAL WEATHER SERVICE
NATIONAL METEOROLOGICAL CENTER

OFFICE NOTE 237

Experiments on the Parameterization of the Flux of Sensible Heat and Moisture from the Sea Surface into the LFM Boundary Layer

John E. Newell
Development Division

JUNE 1981

This is an unreviewed manuscript, primarily intended for informal exchange of information among NMC staff members.

1.) Introduction.

It has frequently been noted that LFM forecasts of boundary layer relative humidity are too low at oceanic locations. It is not unusual for a significant number of gridpoints to drop from a relative humidity of seventy percent or higher to a value less than forty percent within the first six hours of the forecast. By twelve hours or more after initial time, a large number of oceanic points may be found to have a boundary layer relative humidity of thirty percent, which is the minimum value allowed by the model at locations over the sea. This characteristic of the LFM is disturbing because it is so unrealistic.

Another weakness of the model is its slowness in forecasting the onset of precipitation in the strong southerly flow from the Gulf of Mexico or in the easterly flow from the Atlantic. Even when it does forecast precipitation in these cases, it is frequently deficient in the predicted amount. This characteristic of the model has been thought to be related to the lack of a flux of moisture from the ocean into the boundary layer of the LFM.

2.) The 10-Layer LFM Model.

The experiments reported here were conducted not with the operational version of the LFM, which contains seven information levels in the vertical, but with a 10-layer version of the model. This 10-layer LFM is derived from the 7-layer version in a straightforward manner by dividing each of the latter's three tropospheric layers in half. No change is made to the structure above the tropopause, each model containing three stratospheric layers between the tropopause and the 50 mb level. Figure 1 illustrates the structure of the two models between the surface of the earth and the tropopause. The dashed lines in the figure indicate the midpoint of a layer.

In constructing the 10-layer LFM, every effort was made to retain the numerical procedures and the physical parameterizations of the 7-layer. For example, since the 7-layer carries moisture in its three lowest layers, it was decided that the 10-layer would do so in its five lowest layers. The rationale for using the 10-layer model in these experiments is that it was believed that the higher resolution model would be more sensitive to changes in the physical parameterization.

3.) Formulation of the Heat and Moisture Flux Terms in the 10-layer LFM Model.

Sensible heat is transferred from the ocean into the model's boundary layer if the sea surface temperature at the point in question exceeds the boundary layer potential temperature. The tendency of boundary layer potential temperature due to the flux of sensible heat is evaluated by:

$$\frac{\partial \theta_B}{\partial t} = K_H \left(T_S - \theta_B\right) \tag{3.1}$$

where θ_B is the boundary layer potential temperature, T_s the sea surface temperature, and K_H the exchange coefficient for sensible heat. More information on the derivation of this formula may be found in the reference by Gerrity (1977). The operational LFM model uses a value of:

$$K_H = 10^{-4} \text{ sec}^{-1} \tag{3.2}$$

Since T_s is independent of time in equation (3.1), it follows that the quantity $(T_s - \theta_B)$ decays exponentially with time toward a value of zero. With a value of K_H equal to 10^{-4} sec^{-1} the difference $(T_s - \theta_B)$ is reduced by an order of magnitude in 6.4 hours. Because θ_B represents the mean potential temperature in a boundary layer approximately 400 meters deep, this value of K_H seems too large.

The flux of moisture from the sea into the boundary layer is parameterized in a manner quite similar to that employed for the flux of sensible heat. As with the sensible heat flux, moisture is added to the boundary layer only if

$T_S > \theta_B$. Flux of moisture from the sea is not allowed if RH_B, the boundary layer relative humidity, exceeds 70 percent. The reason for this last restriction involves the convective precipitation algorithm of the LFM. A boundary layer relative humidity of 75 percent is required as a necessary condition for convective precipitation originating in the boundary layer. It is not desirable for moisture flux to trigger widespread convective rain at oceanic gridpoints, and it has been observed that this will occur if the moisture flux is allowed to operate when the boundary layer relative humidity is greater than 70 percent.

A value of saturation specific humidity, q_{SST}, corresponding to the sea surface temperature, T_S, is calculated and integrated vertically through the 50 mb deep boundary layer to obtain W_{SST}, the saturation value of boundary layer precipitable water to be used in the calculation of the moisture flux. W_{SST} should not be confused with the saturation value of boundary layer precipitable water, W_{SB}, determined by the boundary layer potential temperature, θ_B. If W_B denotes the actual value of boundary layer precipitable water, then the relative humidity in the boundary layer, RH_B, is defined as:

$$RH_B = \frac{W_B}{W_{SB}} \tag{3.3}$$

If $T_S > \theta_B$, and if $RH_B \leq 70$ percent, then the tendency of boundary layer precipitable water due to flux of moisture from the ocean is evaluated as:

$$\frac{\partial W_B}{\partial t} = K_W \, (W_{SST} - W_B) \tag{3.4}$$

where K_W is the exchange coefficient for flux of water vapor.

4.) The case of 1200Z 18 Feb. 1979.

This is the famous Washington's Birthday storm, which dumped 18 inches of snow on the District of Columbia and larger amounts to the north and east.

Figure 2 shows the initial conditions at sea level. A massive arctic high is centered over northern New York and an inverted trough extends from the Gulf of Mexico northward into the Ohio Valley. The situation 24 hours later is shown in Figure 3. The high pressure cell has moved eastward over the Atlantic and a low center appears off the coast of North Carolina. Manual analysis of the sea level data indicated that the depth of this low was about 1008 mb. Figure 4 displays the sea level analysis 36 hours after initial time. The low center has deepened considerably and moved northeastward.

The observed precipitation amounts for the first 24 hours after 1200Z 18 Feb. 1979 are shown in Figure 5, and for the second 24 hours in Figure 6. The bulk of the second day precipitation actually occurred during the period 1200Z 19 Feb. to 0000Z 20 Feb., so that we may legitimately compare Figure 6 with the forecast model's predictions for that same 12 hour period.

5.) Discussion of Experiments.

The 10-layer LFM model was run from initial data of 1200Z 18 Feb. 1979 in a series of experiments in which the exchange coefficients for sensible heat and for moisture were varied. The values used in the different forecasts are shown in Table 1.

Experiment A may be regarded as the control run, since it uses the same values employed by the operational LFM. Experiment B will define the impact of the sensible heat flux parameterization when it is compared with A. The remaining three experiments test the sensitivity of the model to different values of K_H for a fixed value of K_W. The principal function of a non-zero value of K_W is to transport moisture from the sea into the model's boundary layer. The numerical value chosen determines the rapidity with which a grid-point whose initial boundary layer relative humidity is less than 70 percent rises to a value of 70, at which time the moisture flux is ended. Examination of printed maps of boundary layer relative humidity showed that a value of

EXPERIMENT	K_H (sec^{-1})	K_W (sec^{-1})
A	1.0 E-4	0.0
B	0.0	0.0
C	2.0 E-5	2.0 E-5
D	4.0 E-5	2.0 E-5
E	6.0 E-5	2.0 E-5

Table 1.

$K_W = 2.0$ E-5 sec^{-1} eliminated the problem of drying out during the forecast, which occurred in experiment A. Since this was considered a satisfactory solution, no change was made to the value of K_W in experiments C, D, and E.

Figures 7a to 7e show the forecast 12-hour accumulated precipitation during the first 12 hours after initial time and the 700 mb vertical velocity. The lower case letters of the figures correspond to the capital letters of Table 1. Note that the three runs with moisture flux have an area of precipitation south of Newfoundland which is lacking in 7a and 7b. Elsewhere, the differences are slight.

The 12-hour accumulated precipitation during the second 12-hour period after initial time is shown in figures 8a to 8e. Comparing 8a and 8b, notice how the absence of sensible heat flux diminishes the magnitude of the vertical velocity center east of North Carolina. Proceeding from 8c through 8e, we observe that the increasing value of K_H augments the vertical velocity and the precipitation maximum in the same area. Overall, the forecasts shown in figures 7 and 8 compare favorably with the observed amounts shown in Figure 5.

In figures 9a to 9e we see the predicted sea level pressure fields at 24 hours. By this time the effect of the sensible heat flux has become significant. In the forecast in 9a we have a 1009 mb low a short distance off the North Carolina coast, while 9b shows an inverted trough in that area. At the location where the low in 9a is situated, the pressure is about 10 mb less than it is in 9b.

The impact of sensible heat is clearly shown by the thickness lines. For example, in 9b the 522 thickness isopleth passes through central New Jersey, while in 9a it is over Massachusetts. The 534 to 540 thickness channel, used to delineate heavy snow areas, is south of the Delmarva peninsula in 9b, but centered over that location in 9a. There is a steady drop in the value of the central pressure of the low center east of North Carolina, as we proceed from 9c to 9e. Note that 9a and 9e are quite similar.

At 36 hours, the comments made on the earlier forecasts are still valid, but more so. Figures 10a through 10e display the 12-hour accumulated precipitation for the third 12-hour period after the initial time. The inclusion of sensible heat flux (10a) changes the precipitation maximum by more than one inch, compared to the forecast without it (10b). The vertical motion is correspondingly increased as well. In figures 10c through 10e, there is a steady growth of precipitation intensity with increasing values of K_H. The impact of the moisture flux parameterization is best seen by comparing 10a and 10e. The latter, with a value of K_H only 60 percent that of the former, has a larger precipitation maximum. This we attribute to the presence of moisture flux in 10e. Experiments A and E are seen to be superior to the other three in capturing the precipitation amounts shown in figure 6.

The 36-hour sea level predictions are seen in figures 11a through 11e. The forecast with sensible heat flux (11a) is greatly superior to the one made without it (11b) in handling the low center shown near 68 degrees west longitude in figure 4, the verifying analysis. Figures 11c through 11e portray the usual increase in cyclone intensity with increasing K_H. Again, it may be noted that experiments A and E are quite similar in their results and are superior to the other three.

6) Conclusions and Recommendations.

The important role played by the flux of sensible heat from the ocean has been shown by a comparison of the results of experiments A and B. By 24 hours after initial time, the two sea level pressure predictions are significantly different in their handling of an important coastal storm. At 36 hours, the circulation differences have had a marked effect on the forecast precipitation as well. The inclusion of sensible heat flux from the ocean into the model atmosphere is clearly beneficial in the case discussed. The sensitivity of the forecast model to the value of the exchange coefficient for sensible heat has been demonstrated for both circulation and precipitation by the results of experiments C, D, and E.

The disturbing drying out of the boundary layer in areas where cold air flows over warm water has been eliminated by the use of a simple parameterization of the flux of water vapor from ocean to atmosphere. Comparison of experiments A and E suggests that inclusion of the moisture flux in the model enables one to use a lower and perhaps more realistic value of the sensible heat exchange coefficient, K_H. Including moisture flux in the model will probably do little to alleviate the slowness in forecasting the onset of precipitation in cases of onshore flow, because the LFM must generate the necessary circulation to produce vertical motion.

As a result of these experiments, further testing of the 10-layer LFM on other cases should be carried out. Experience with the 1200Z 18 Feb. 1979 storm suggests that K_H = 6.0 E-5 sec^{-1} and K_W = 2.0 E-5 sec^{-1} would be appropriate values for the exchange coefficients for sensible heat and water vapor.

Reference

Gerrity, J. P., 1977: The LFM Model--1976: A Documentation. NOAA Technical Memorandum NWS NMC 60.

example, since the 7-layer carries moisture in its three lowest layers, it was decided that the 10-layer would do so in its five lowest layers. The rationale for using the 10-layer model in these experiments is that it was believed that the higher resolution model would be more sensitive to changes in the physical parameterization.

3.) Formulation of the Heat and Moisture Flux Terms in the 10-layer LFM Model.

Sensible heat is transferred from the ocean into the model's boundary layer if the sea surface temperature at the point in question exceeds the boundary layer potential temperatures. The tendency of boundary layer potential temperature due to the flux of sensible heat is evaluated by:

$$\frac{\partial \theta_B}{\partial t} = K_H \, (T_S - \theta_B) \tag{3.1}$$

where θ_B is the boundary layer potential temperature, T_s the sea surface temperature, and K_H the exchange coefficient for sensible heat. More information on the derivation of this formula may be found in the reference by Gerrity (1977). The operational LFM model uses a value of:

$$K_H = 10^{-4} \text{ sec}^{-1} \tag{3.2}$$

Since T_s is independent of time in equation (3.1), it follows that the quantity $(T_s - \theta_B)$ decays exponentially with time toward a value of zero. With a value of K_H equal to 10^{-4} sec^{-1} the difference $(T_s - \theta_B)$ is reduced by an order of magnitude in 6.4 hours. Because θ_B represents the mean potential temperature in a boundary layer approximately 400 meters deep, this value of K_H seems too large.

The flux of moisture from the sea into the boundary layer is parameterized in a manner quite similar to that employed for the flux of sensible heat. As with the sensible heat flux, moisture is added to the boundary layer only if

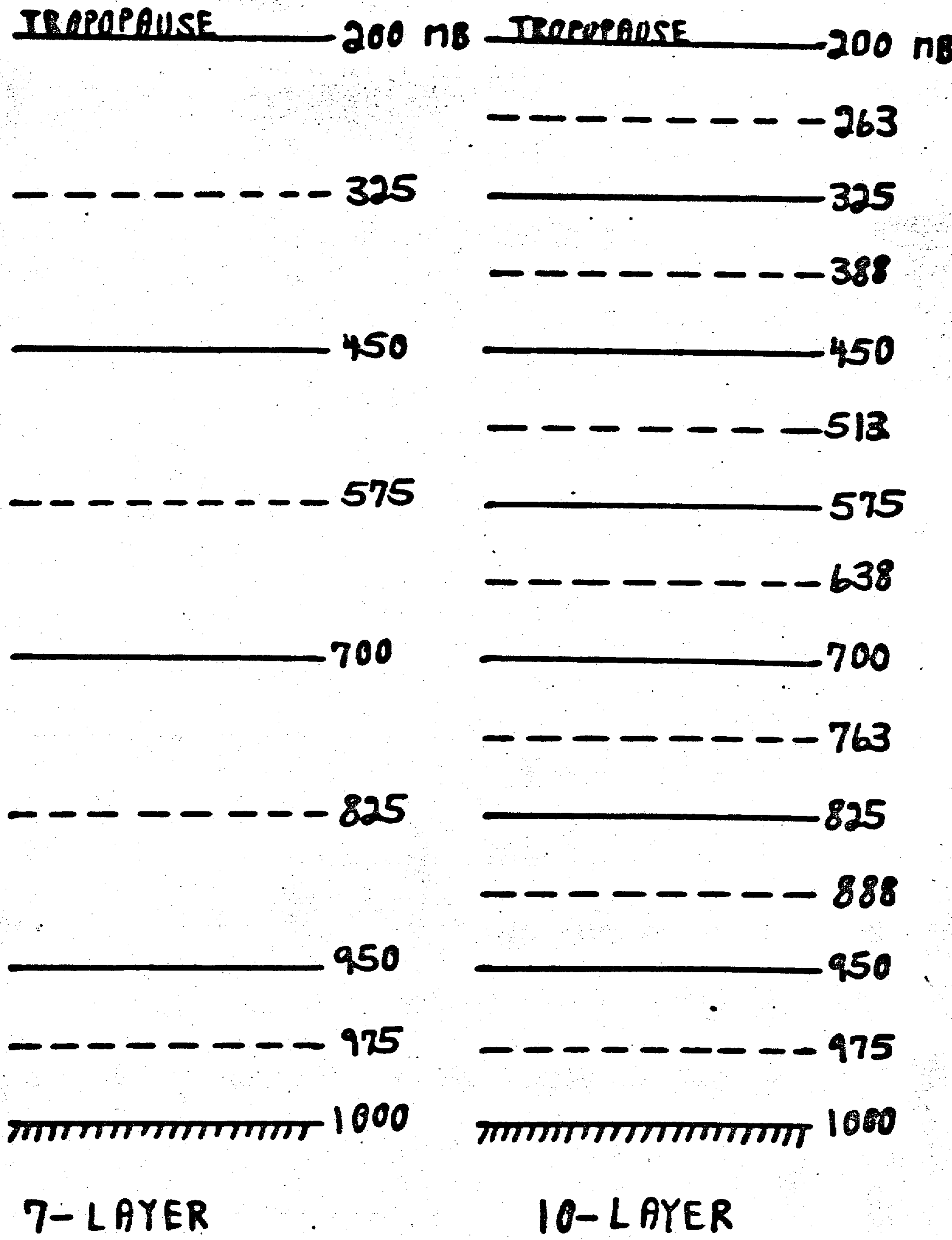
TROPOPAUSE
200 MB
325
450
575
700
825
950
975
1000
7-LAYER
TROPOPAUSE
200 MB
263
325
388
450
513
575
638
700
763
825
888
950
975
1000
10-LAYER

FIGURE 1

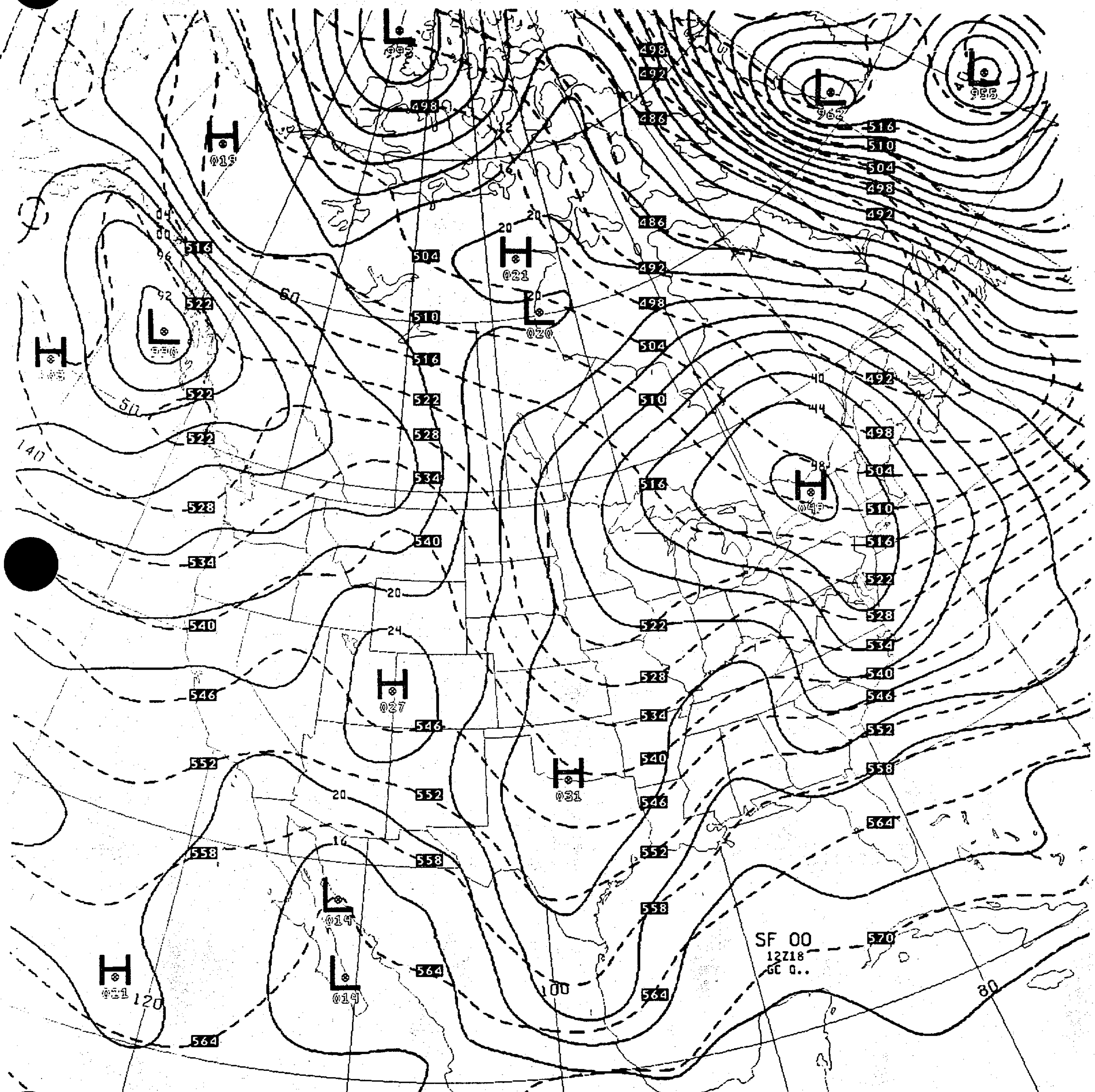

ANALYSIS SFC/1000-500 THICKNESS 12Z SUN 18 FEB 1979 LFM09

FIGURE 2

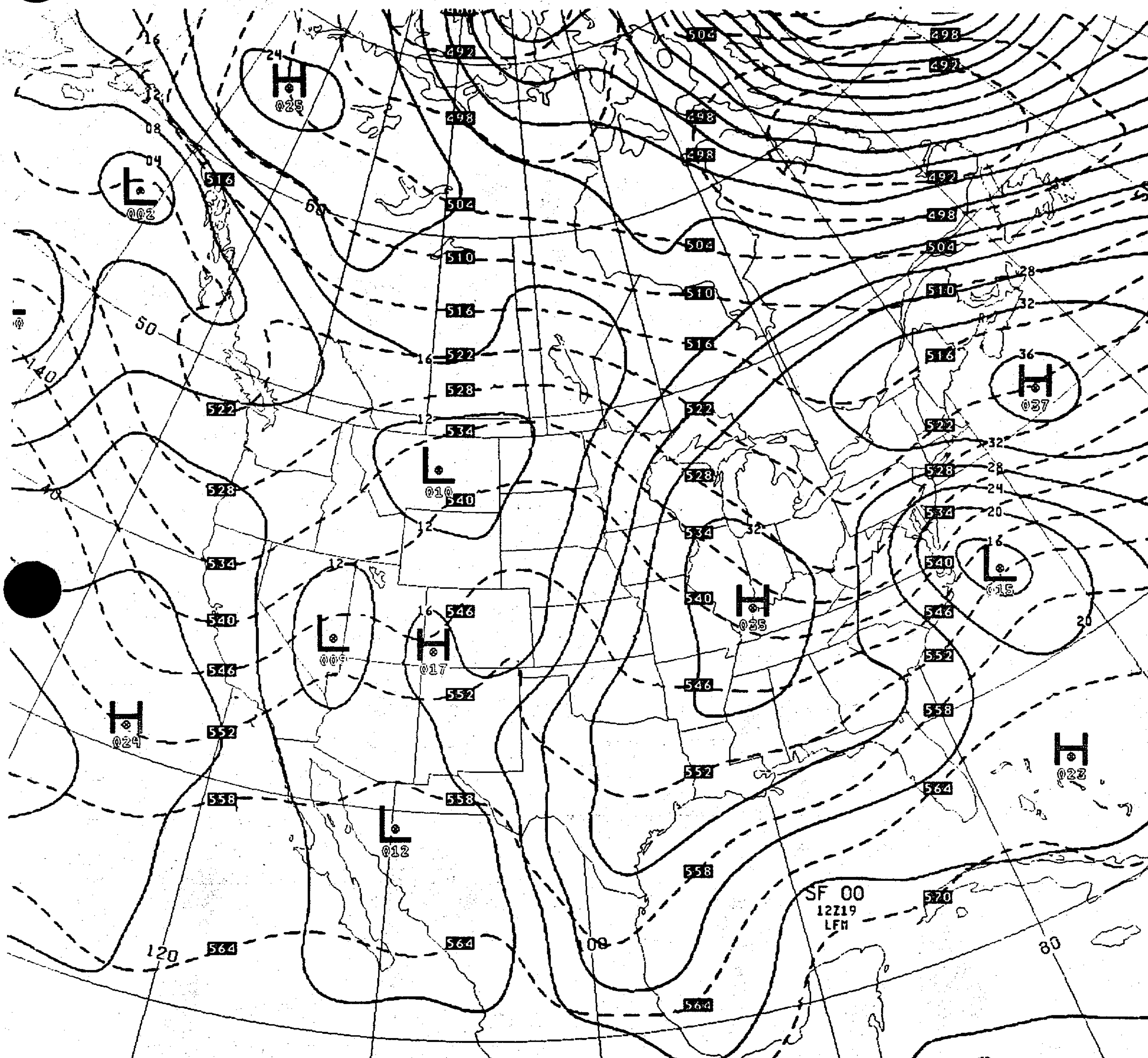

ANALYSIS SFC/1000-500 THICKNESS 12Z MON 19 FEB 1979 LFM09

FIGURE 3

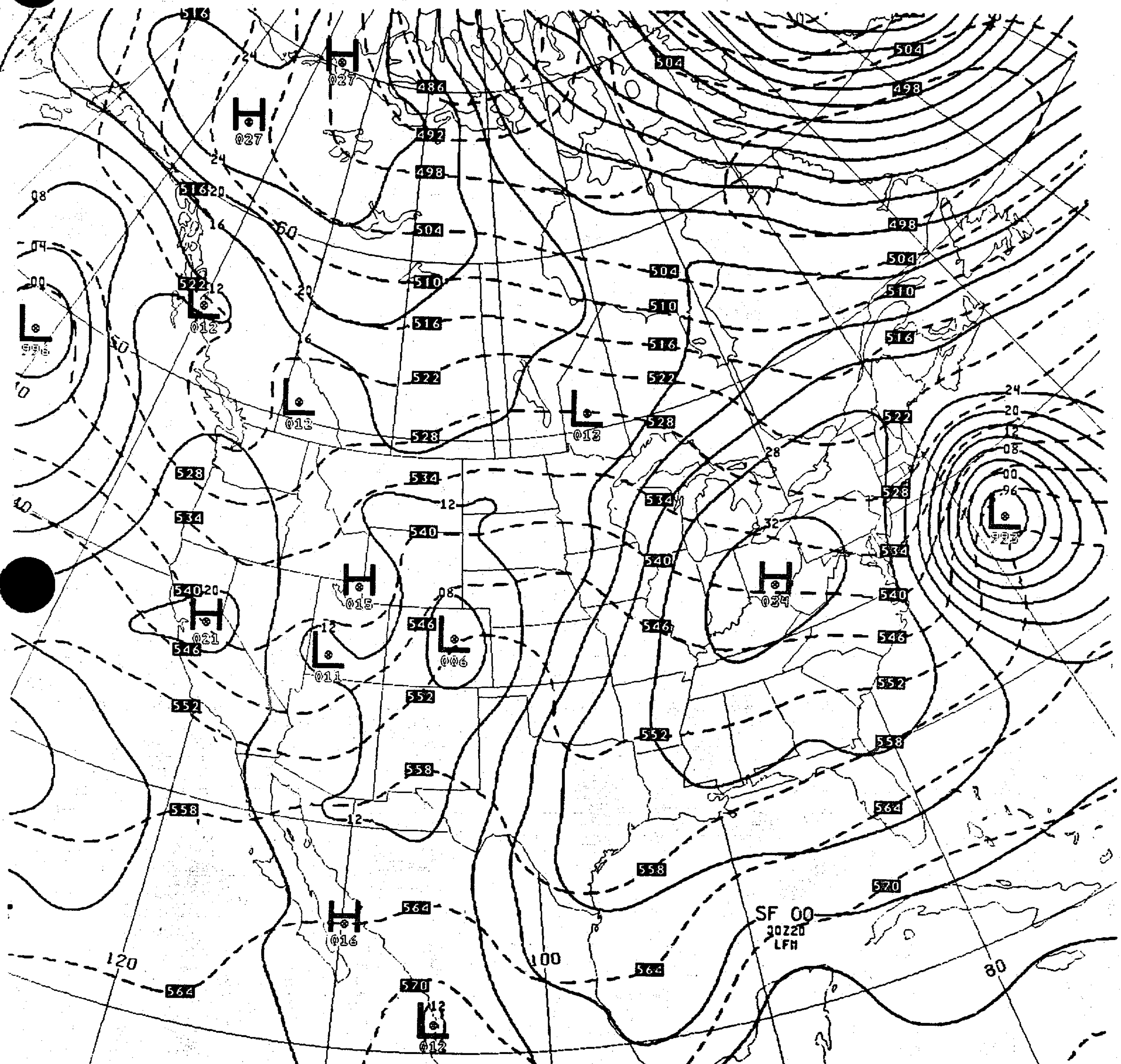

ANALYSIS SFC/1000-500 THICKNESS 00Z TUE 20 FEB 1979 LFM09

FIGURE 4

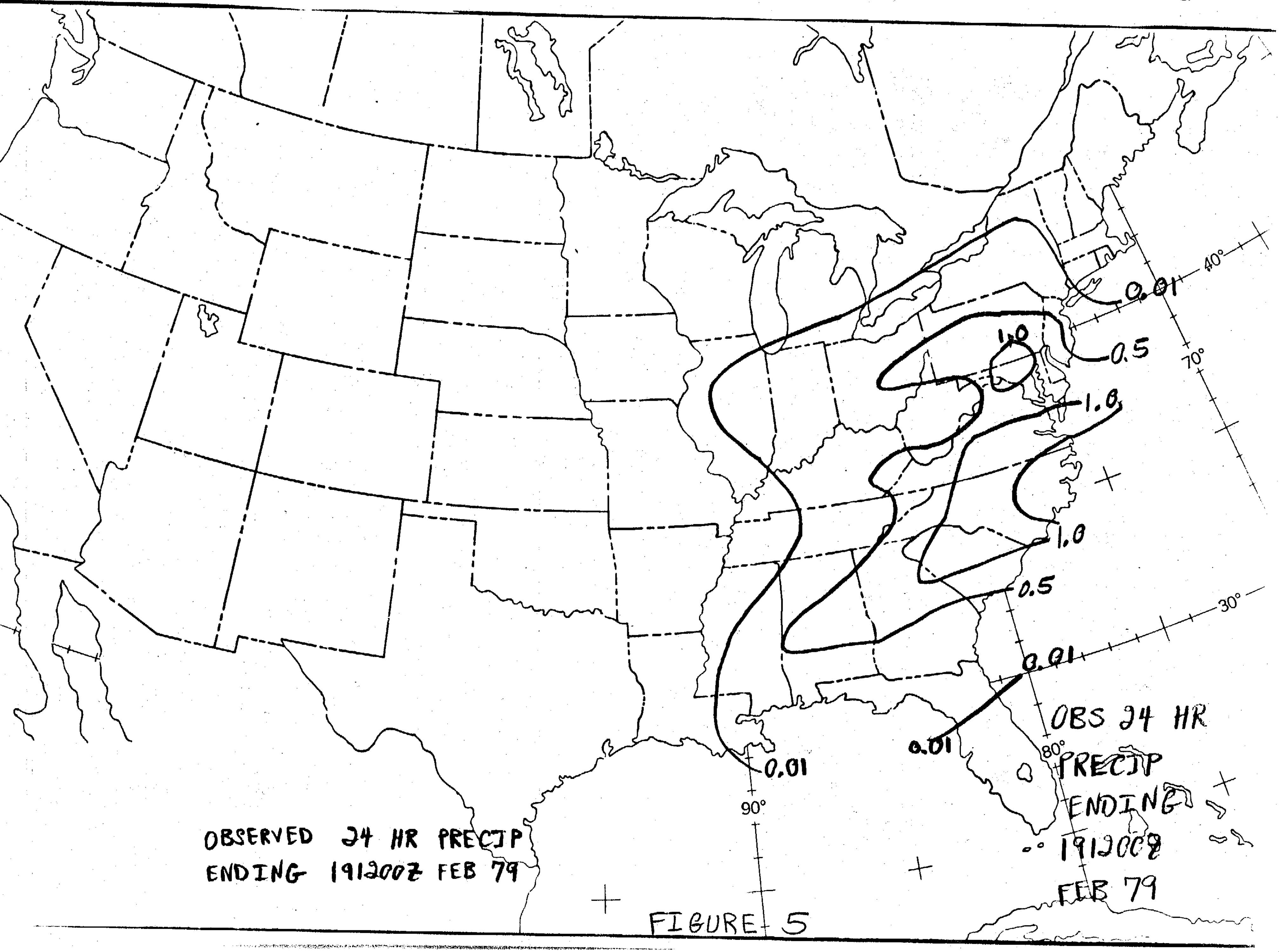
0.01
0.5
1.0
1.0
1.0
0.5
0.01
0.01
0.01
40°
30°
70°
80°
90°
OBS 24 HR PRECIP ENDING 191200Z FEB 79
OBSERVED 24 HR PRECIP ENDING 191200Z FEB 79

FIGURE 5

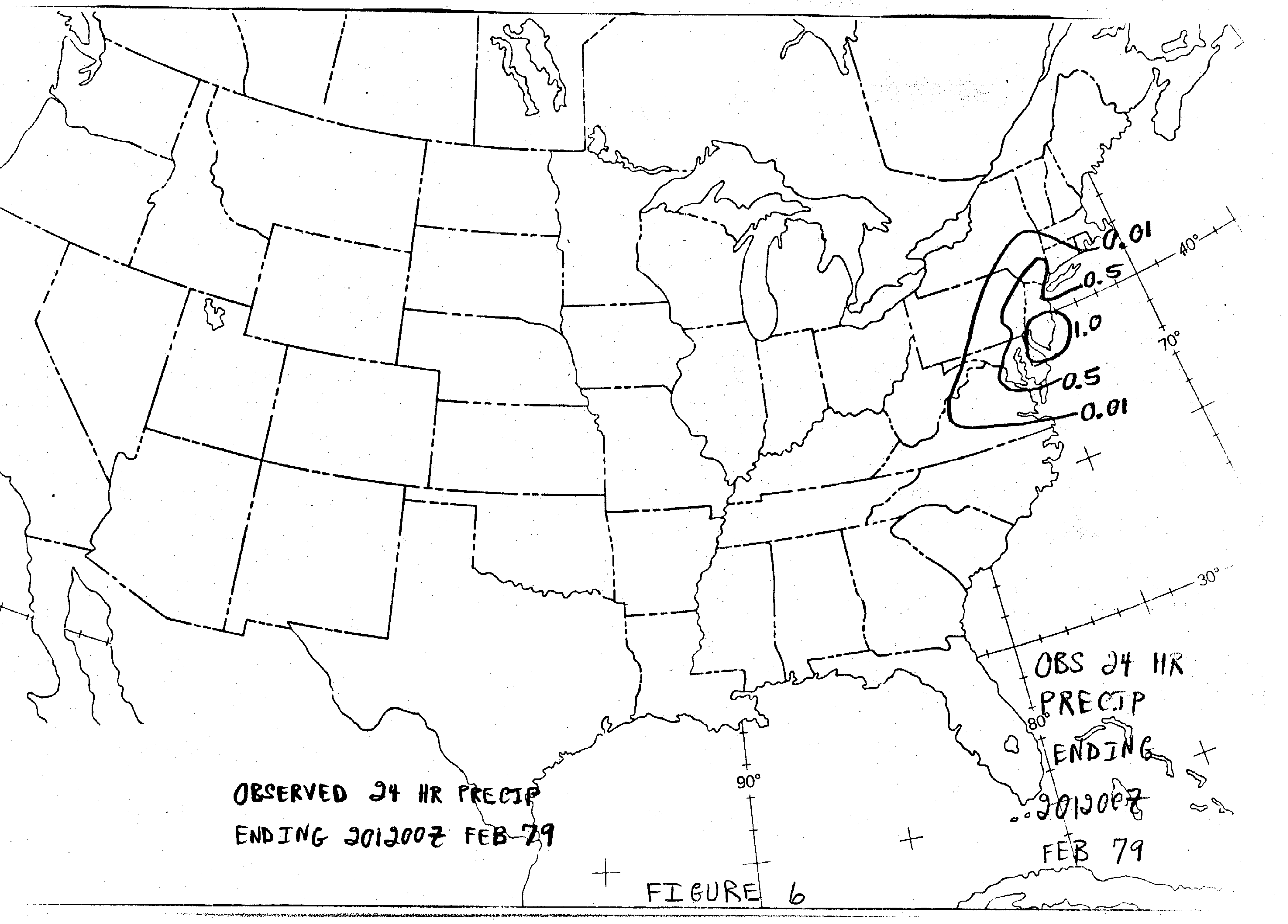

OBSERVED 24 HR PRECIP
ENDING 201200Z FEB 79

FIGURE 6

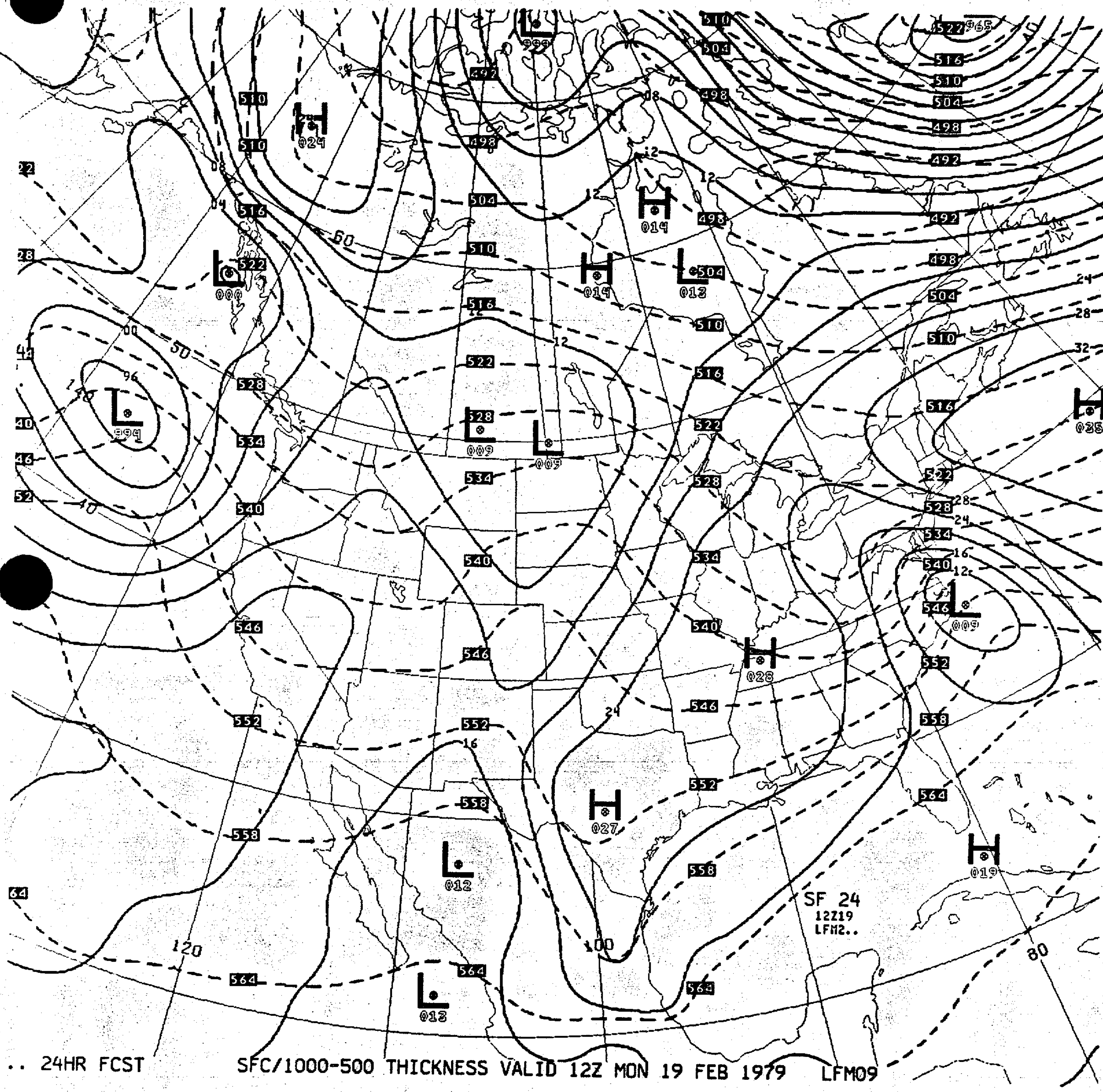
SF 24
12Z19
LFM2..
.. 24HR FCST
SFC/1000-500 THICKNESS VALID 12Z MON 19 FEB 1979
LFM09

FIGURE 9e

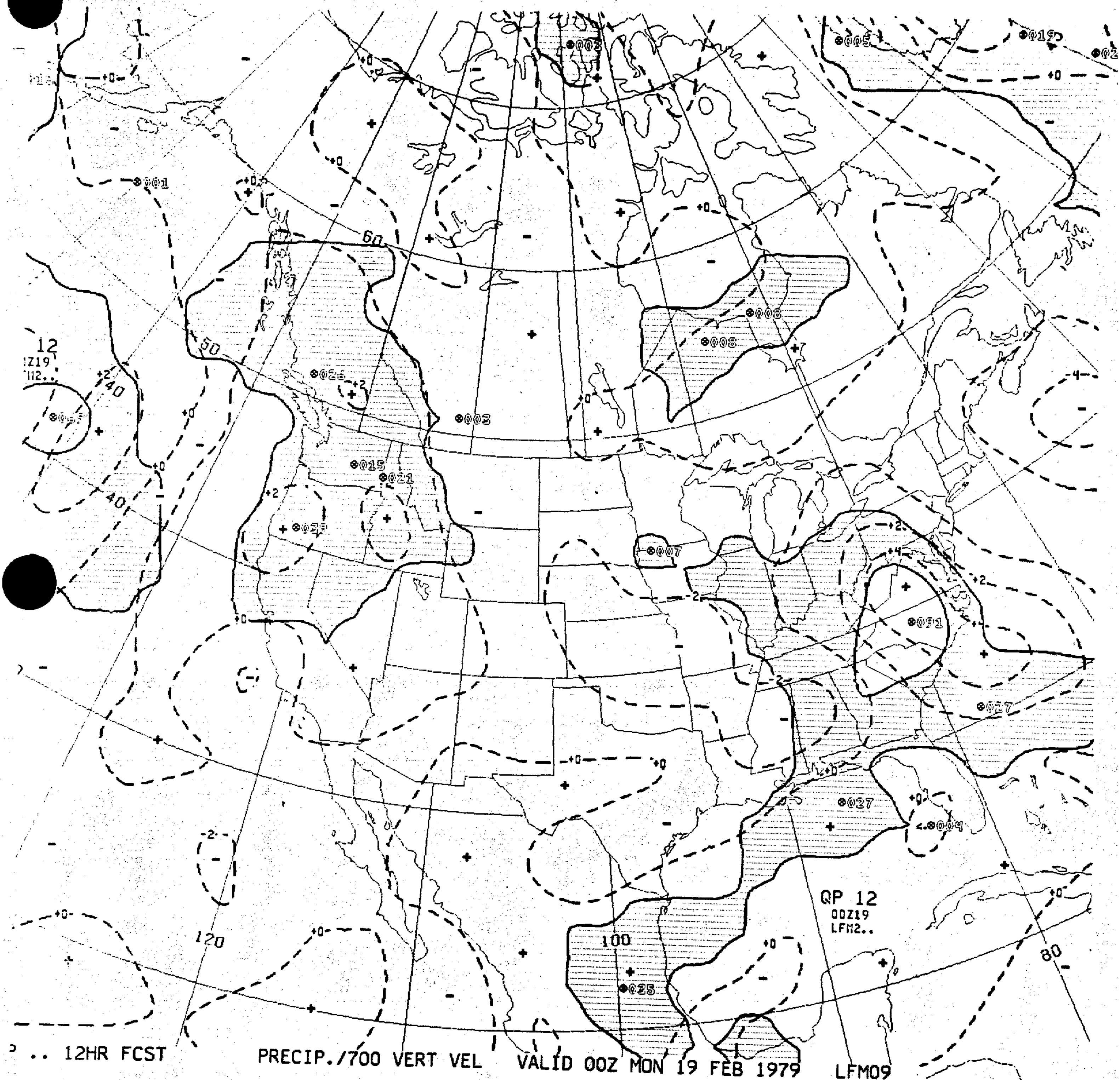
QP 12
00Z19
LFM2..
12HR FCST
PRECIP./700 VERT VEL
VALID 00Z MON 19 FEB 1979
LFM09

FIGURE 7a

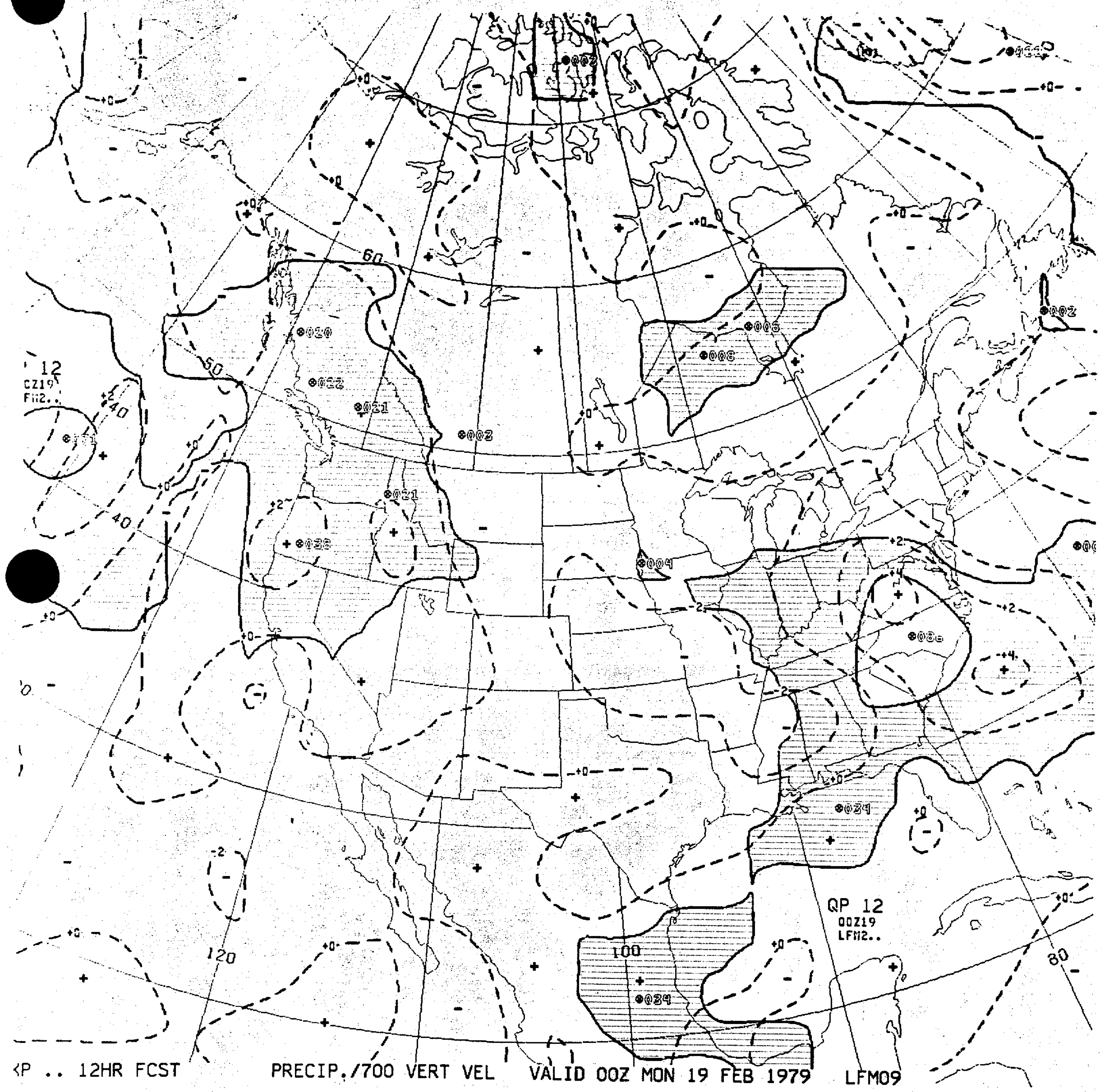

12
CZ19
FH2..
60
50
40
120
100
80
QP 12
00Z19
LFM2..
KP .. 12HR FCST
PRECIP./700 VERT VEL
VALID 00Z MON 19 FEB 1979
LFM09

FIGURE 7b

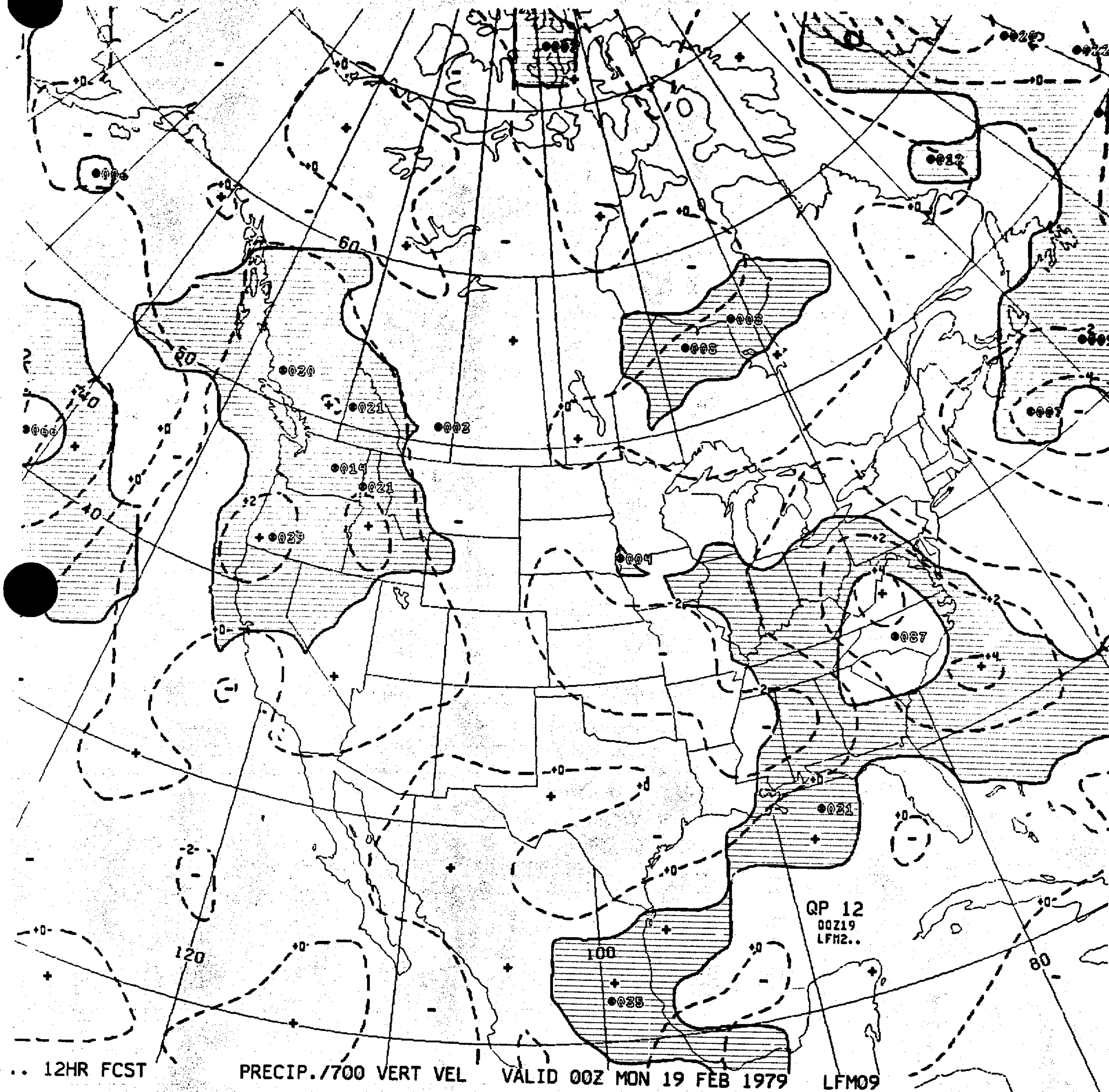

.. 12HR FCST PRECIP./700 VERT VEL VALID 00Z MON 19 FEB 1979 LFM09

FIGURE 7c

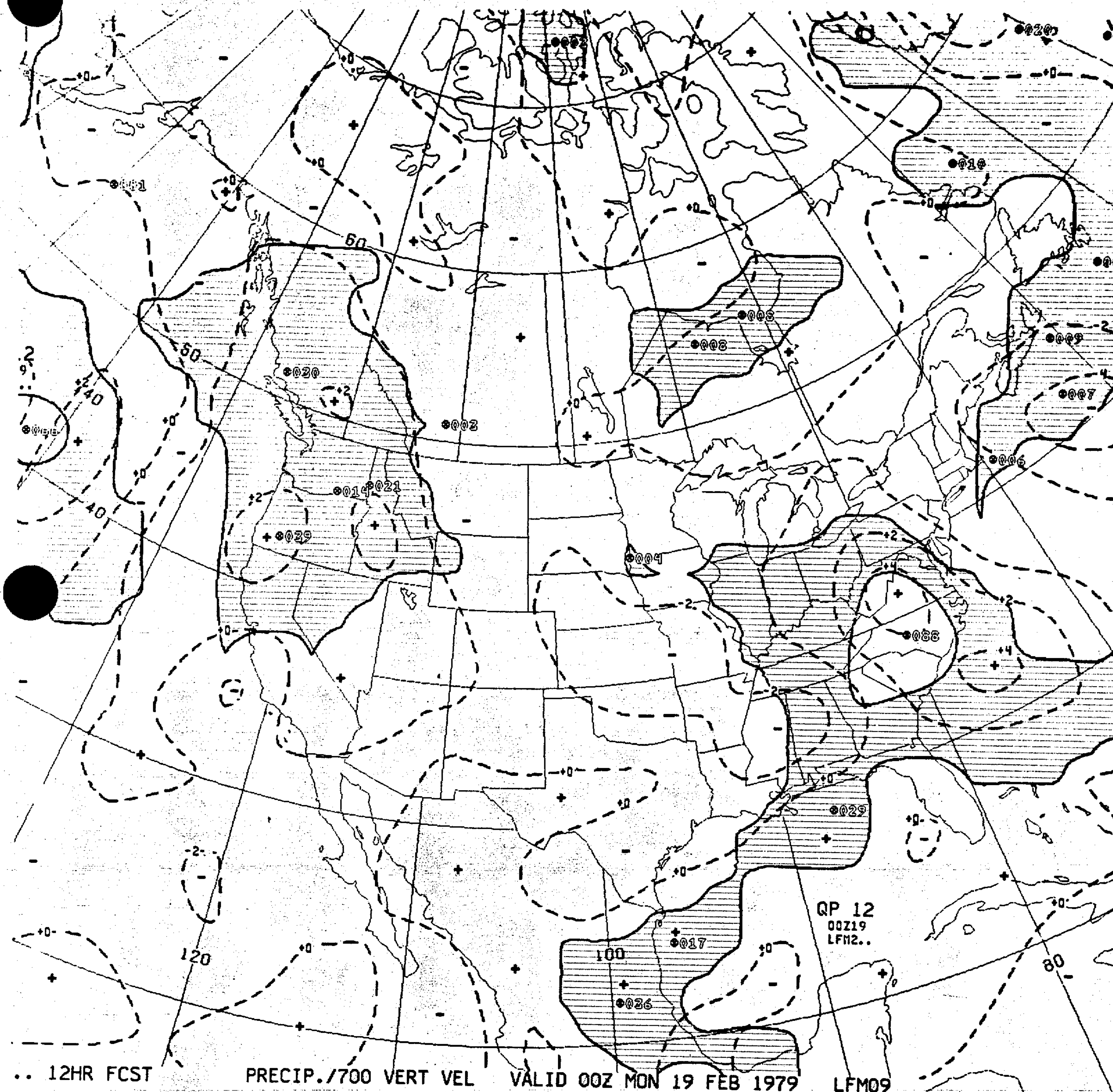
QP 12
00Z19
LFM2..
.. 12HR FCST PRECIP./700 VERT VEL VALID 00Z MON 19 FEB 1979 LFM09

FIGURE 7d

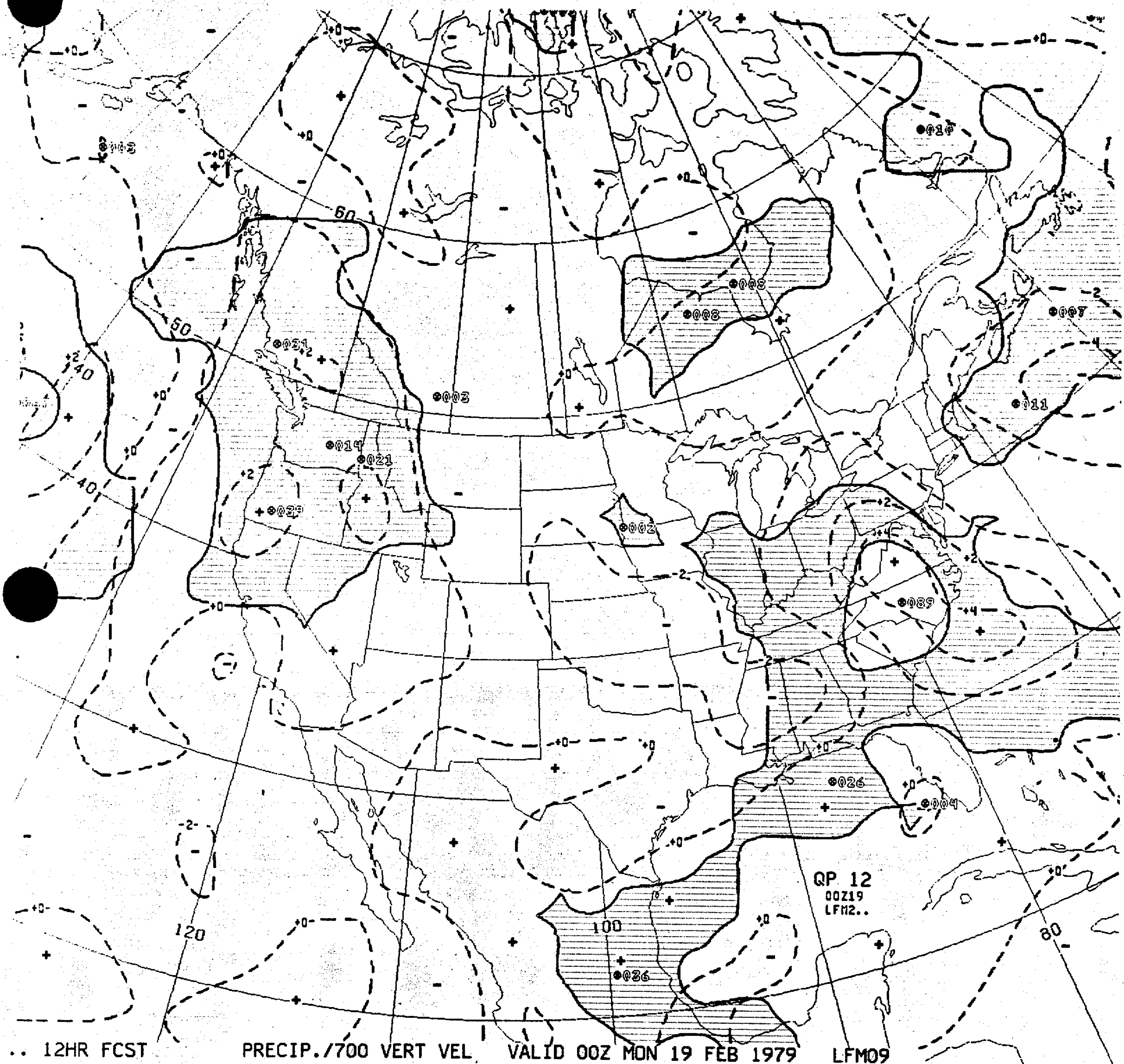
QP 12
00Z19
LFM2..
.. 12HR FCST PRECIP./700 VERT VEL VALID 00Z MON 19 FEB 1979 LFM09

FIGURE 7e

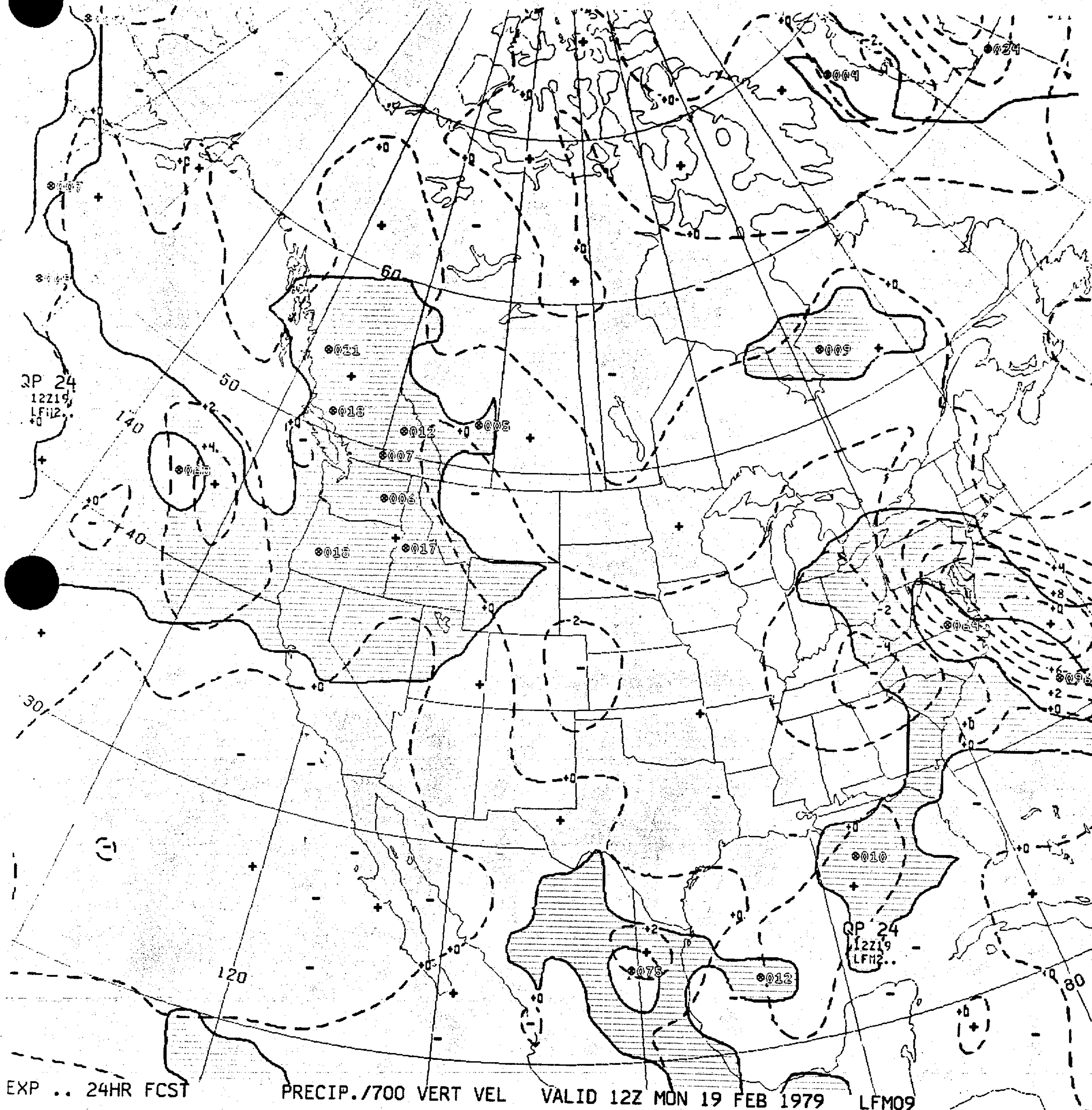
QP 24
12Z19
LFM2..
EXP .. 24HR FCST PRECIP./700 VERT VEL VALID 12Z MON 19 FEB 1979 LFM09

FIGURE 8a

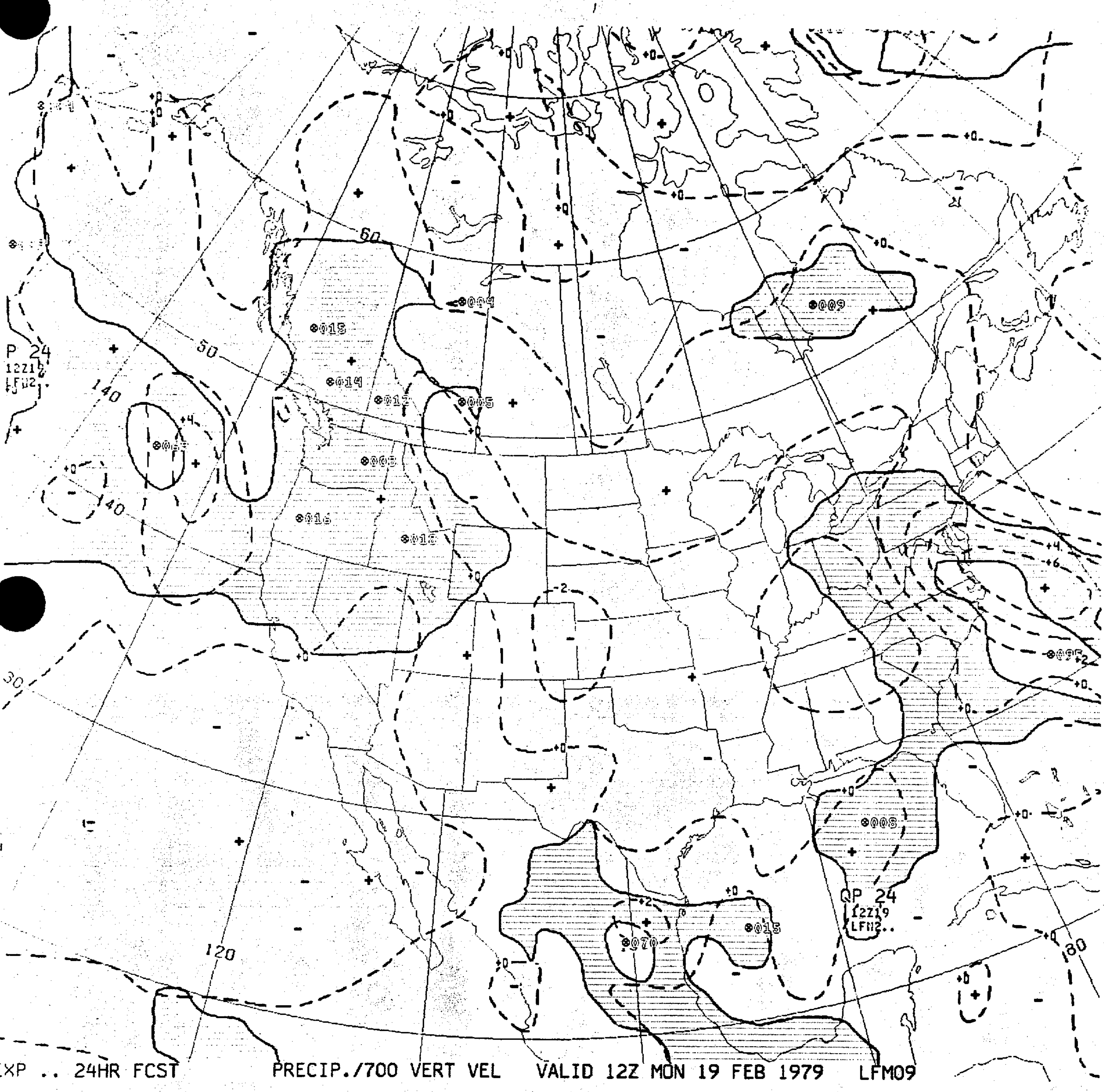
EXP .. 24HR FCST
PRECIP./700 VERT VEL
VALID 12Z MON 19 FEB 1979
LFM09
QP 24
12Z19
LFM2..
60
50
40
30
140
120
80

FIGURE 8b

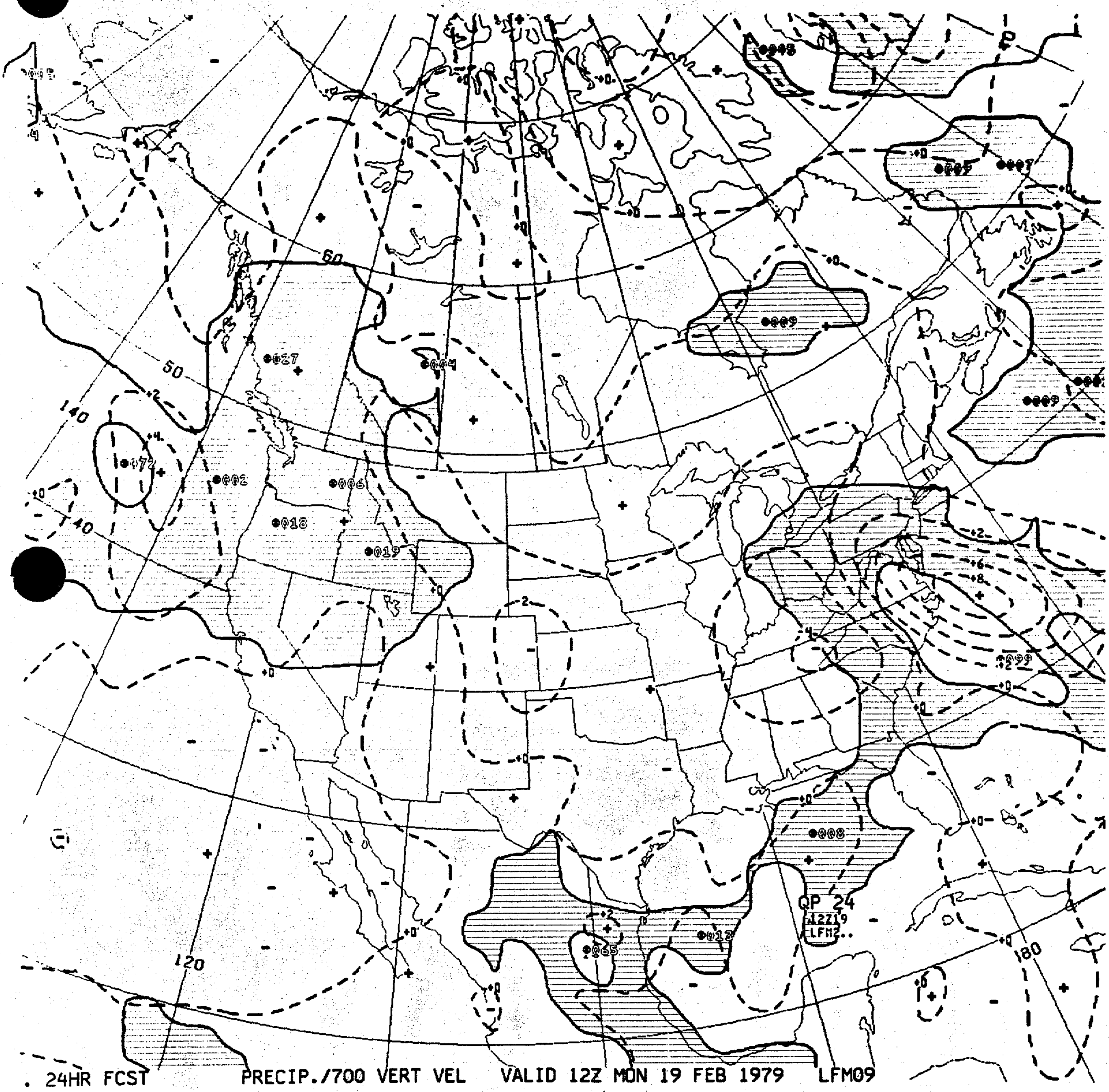

. 24HR FCST PRECIP./700 VERT VEL VALID 12Z MON 19 FEB 1979 LFM09
QP 24

FIGURE 8c

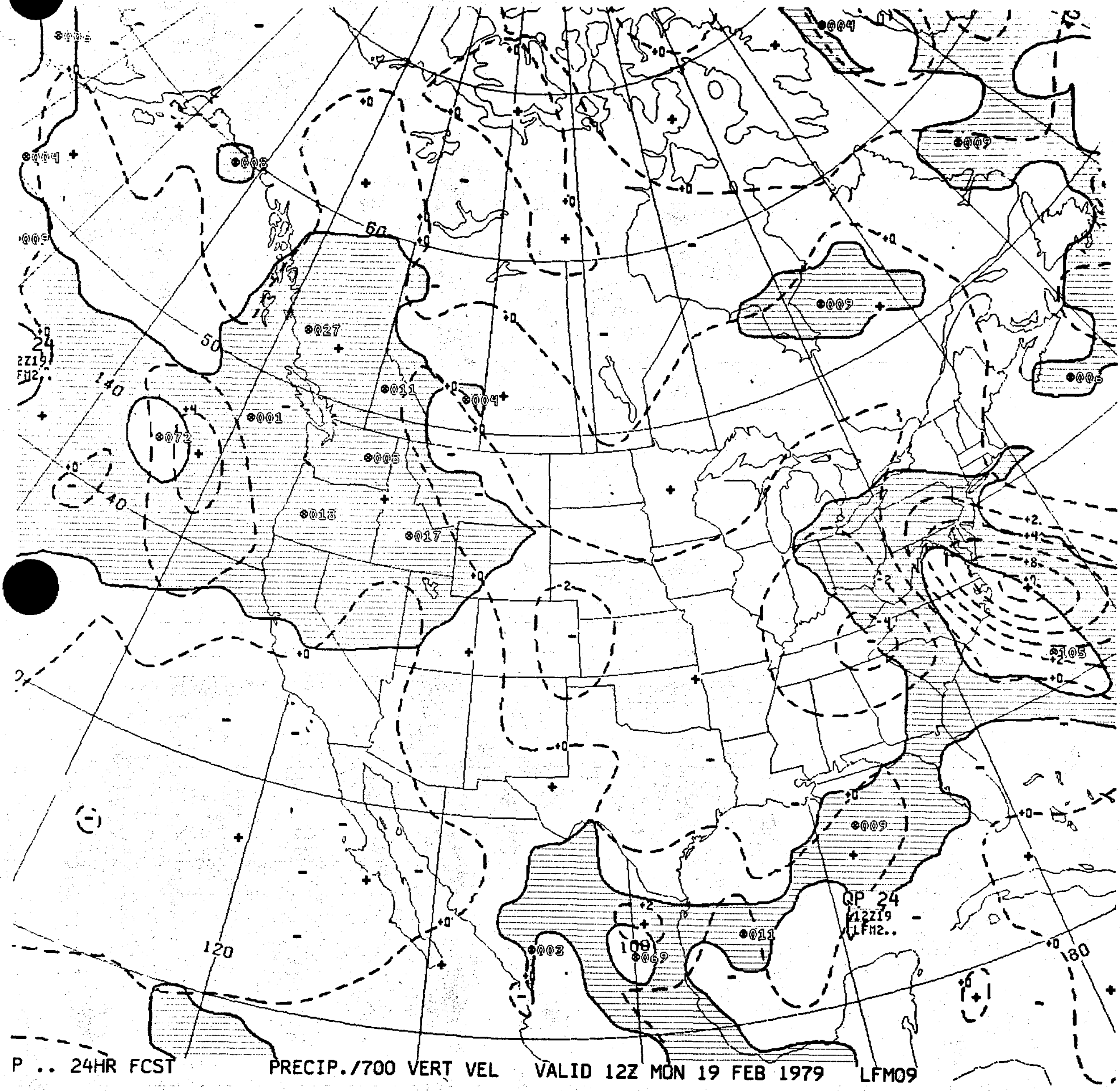

P .. 24HR FCST PRECIP./700 VERT VEL VALID 12Z MON 19 FEB 1979 LFM09

FIGURE 8d

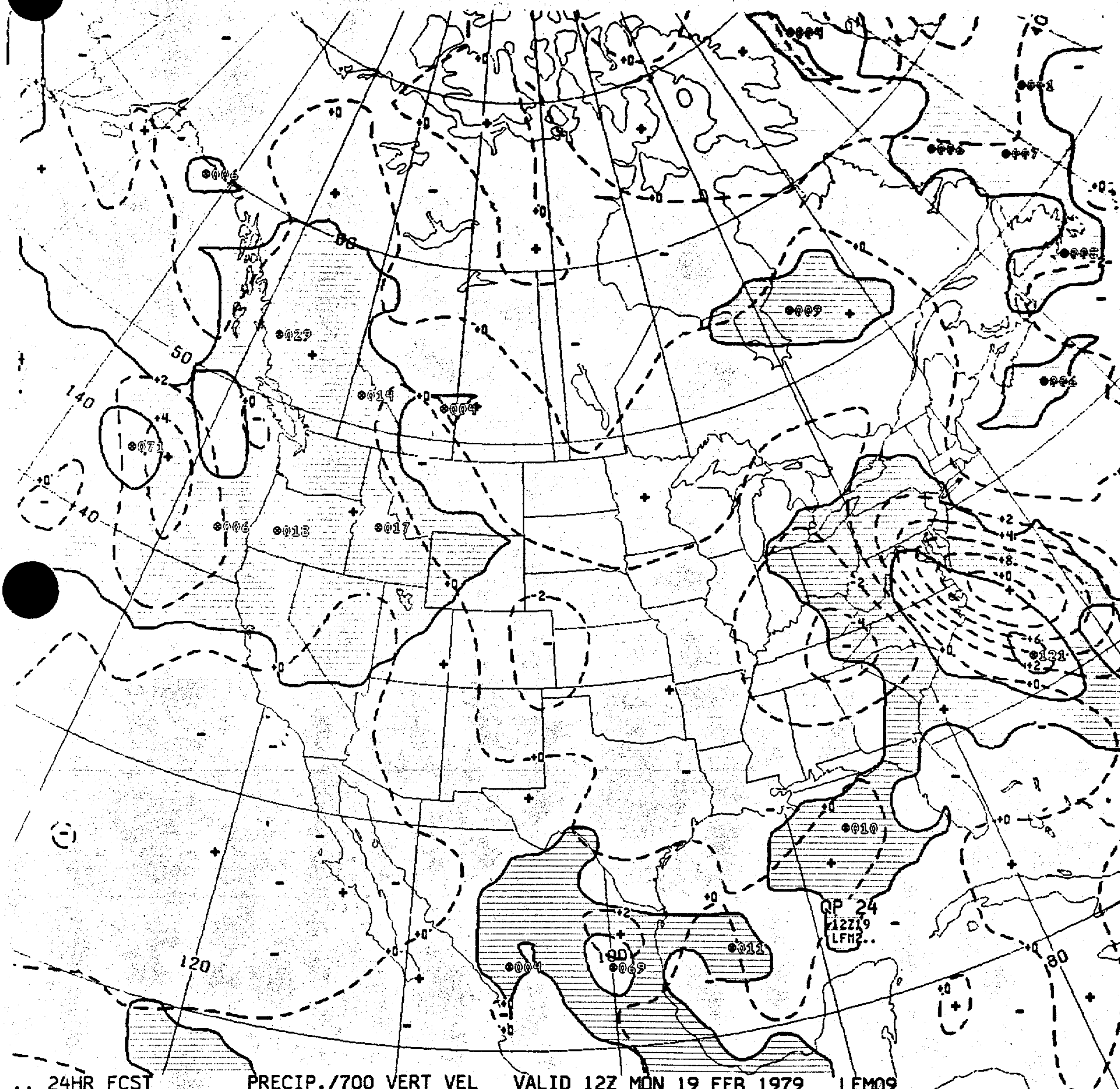
.. 24HR FCST PRECIP./700 VERT VEL VALID 12Z MON 19 FEB 1979 LFM09
QP 24

FIGURE 8e

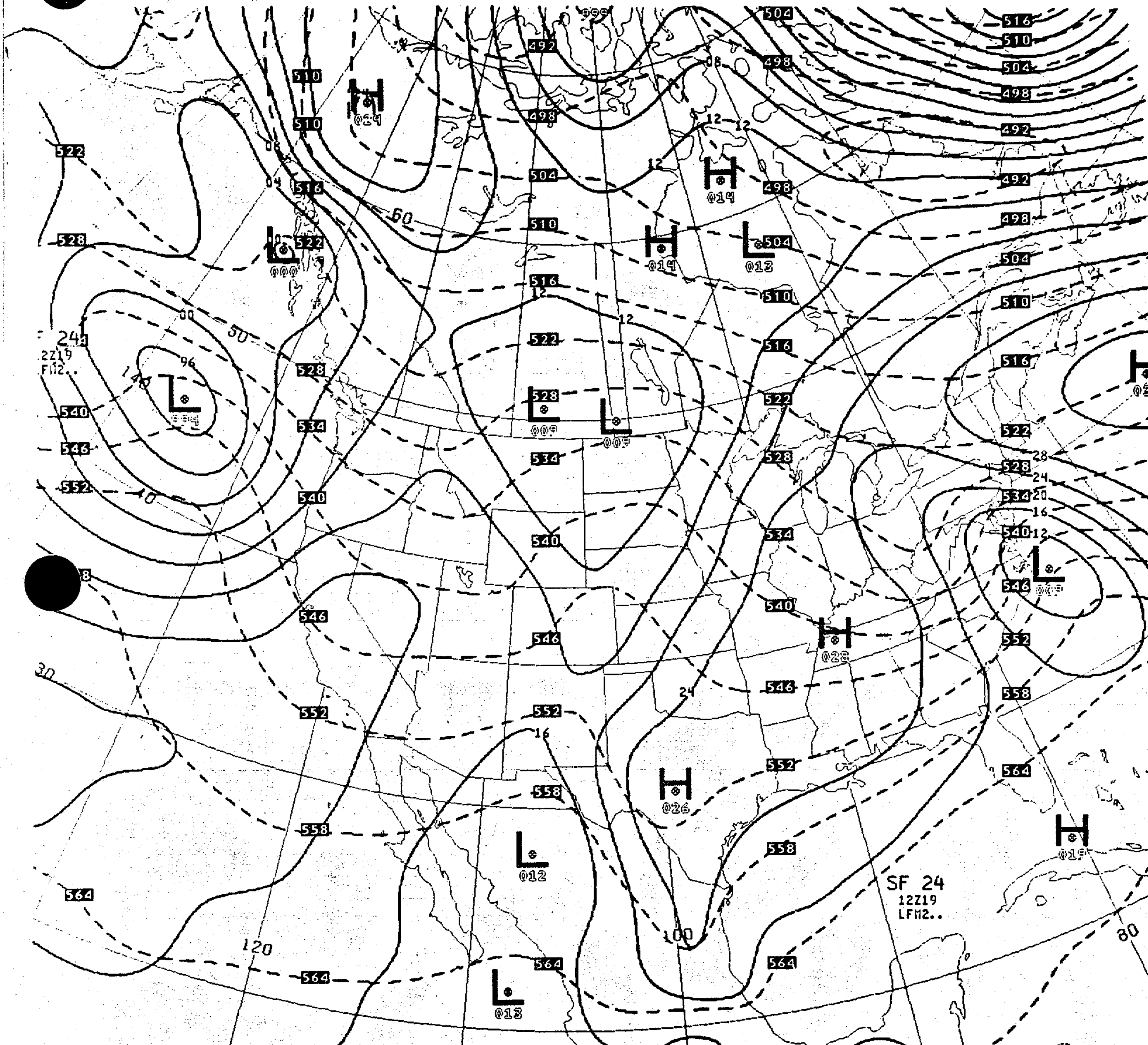

EXP .. 24HR FCST SFC/1000-500 THICKNESS VALID 12Z MON 19 FEB 1979 LFM09

FIGURE 9a

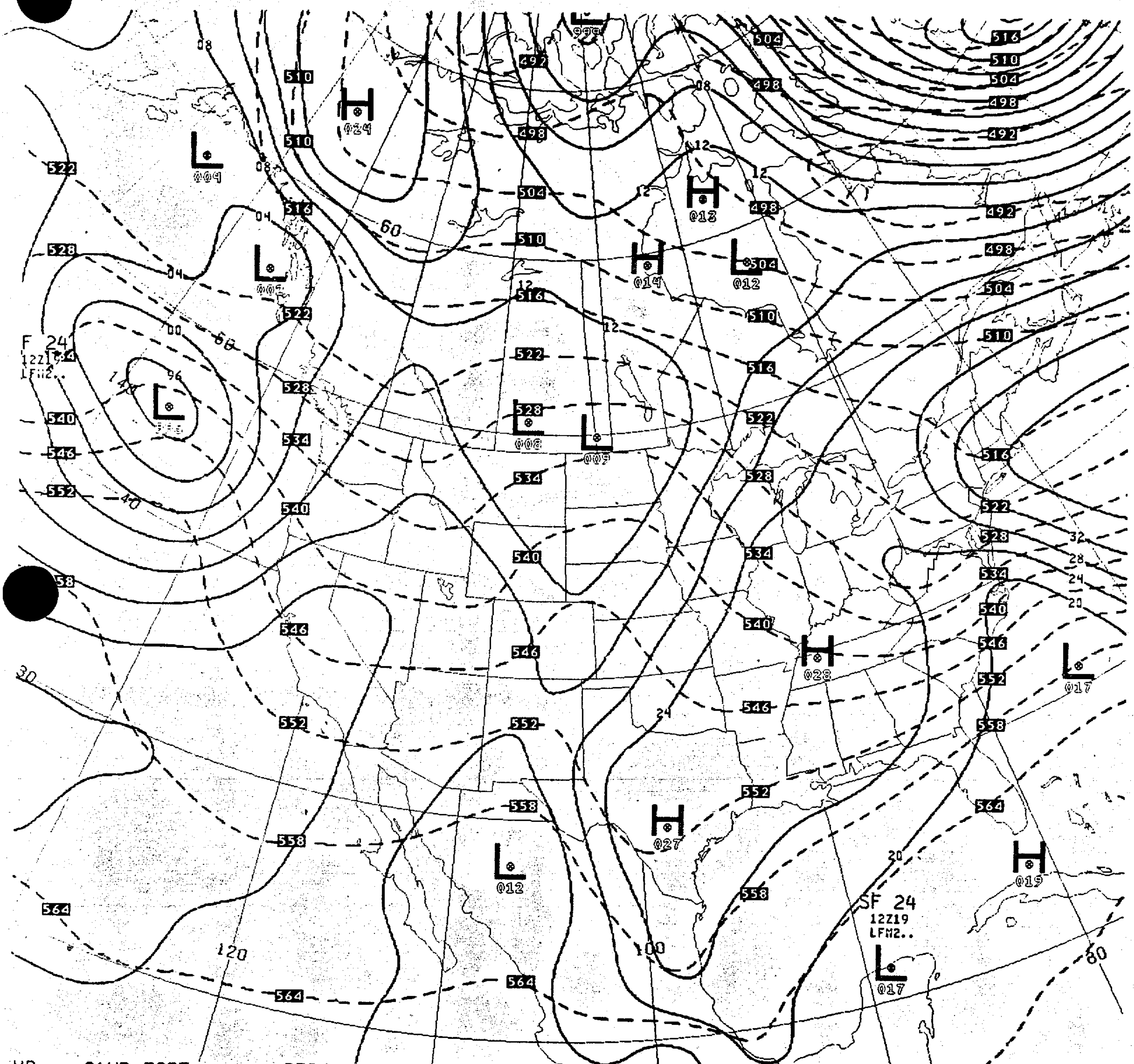

XP .. 24HR FCST SFC/1000-500 THICKNESS VALID 12Z MON 19 FEB 1979 LFM09

FIGURE 9b

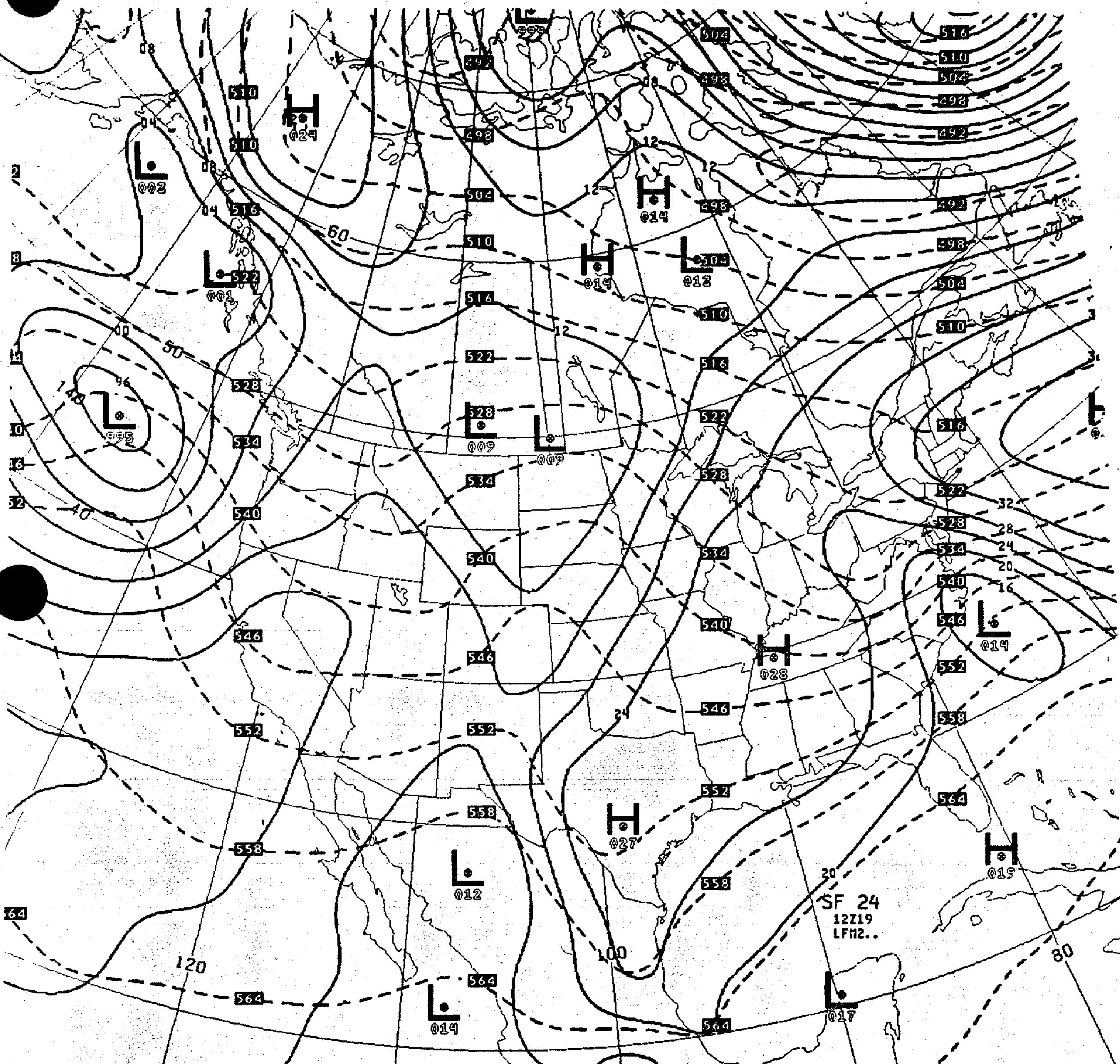

.. 24HR FCST SFC/1000-500 THICKNESS VALID 12Z MON 19 FEB 1979 LFM09

FIGURE 9c

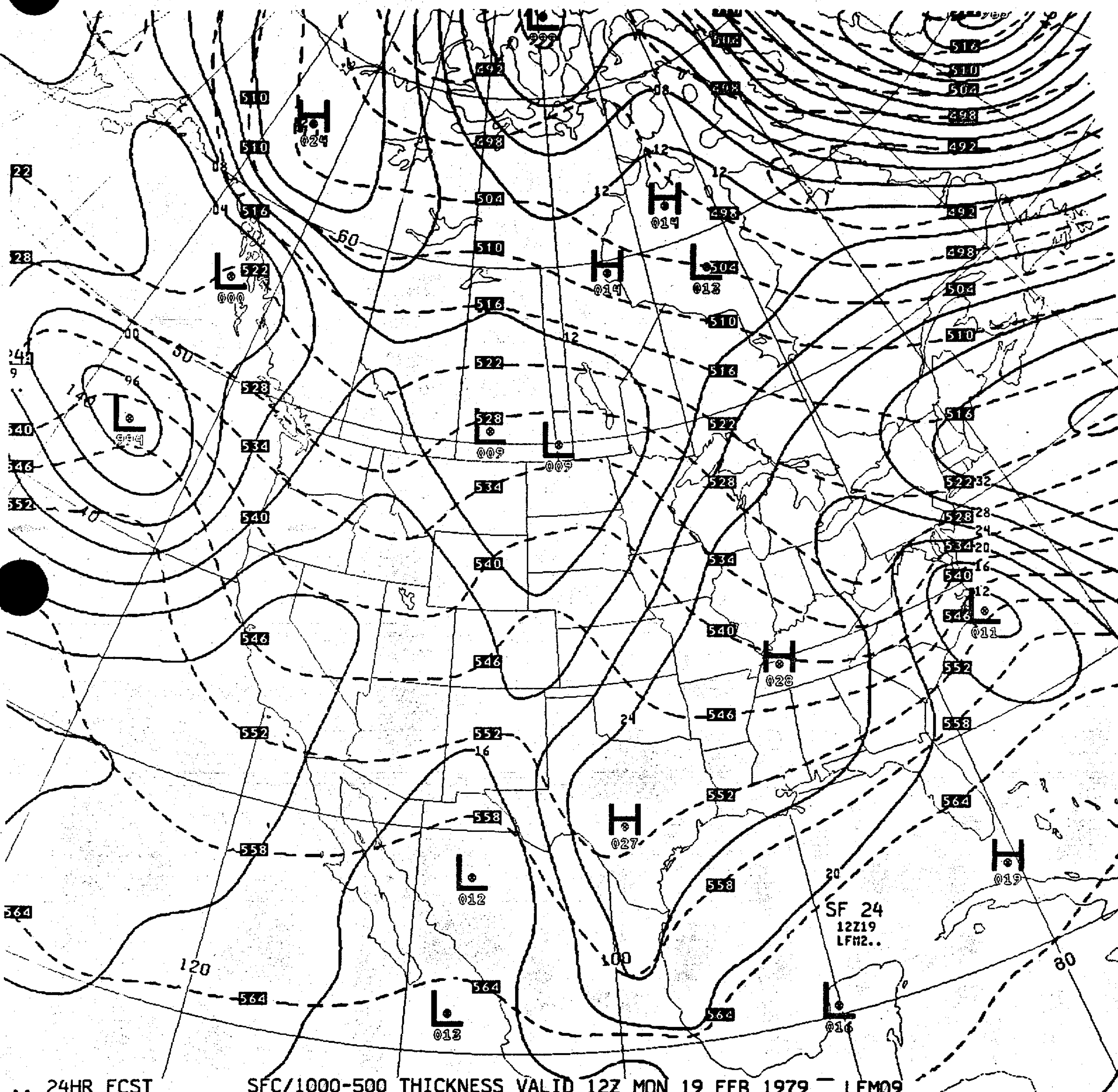

.. 24HR FCST SFC/1000-500 THICKNESS VALID 12Z MON 19 FEB 1979 LFM09

FIGURE 9d

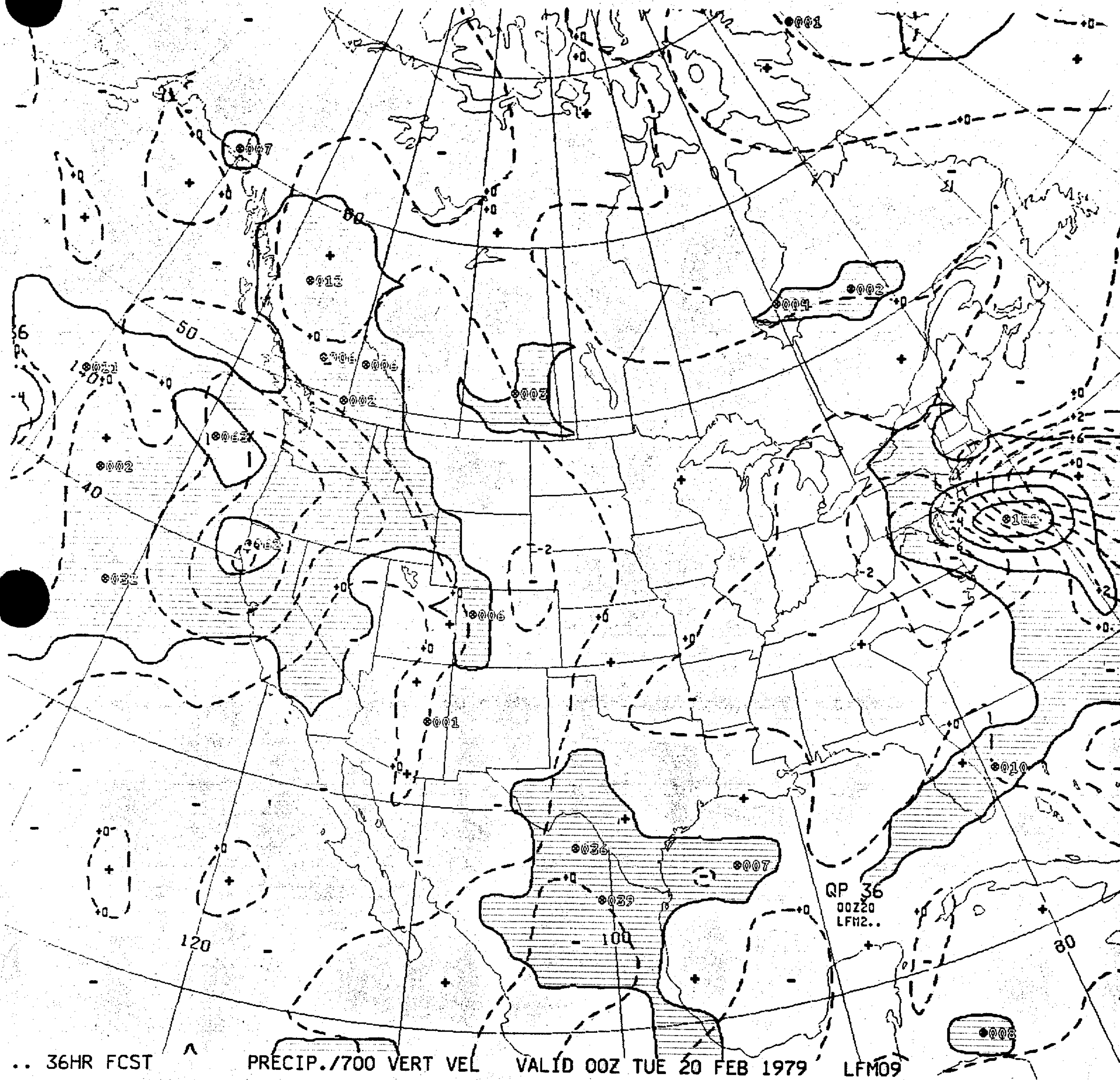
QP 36
00Z20
LFM2..
.. 36HR FCST PRECIP./700 VERT VEL VALID 00Z TUE 20 FEB 1979 LFM09

FIGURE 10a

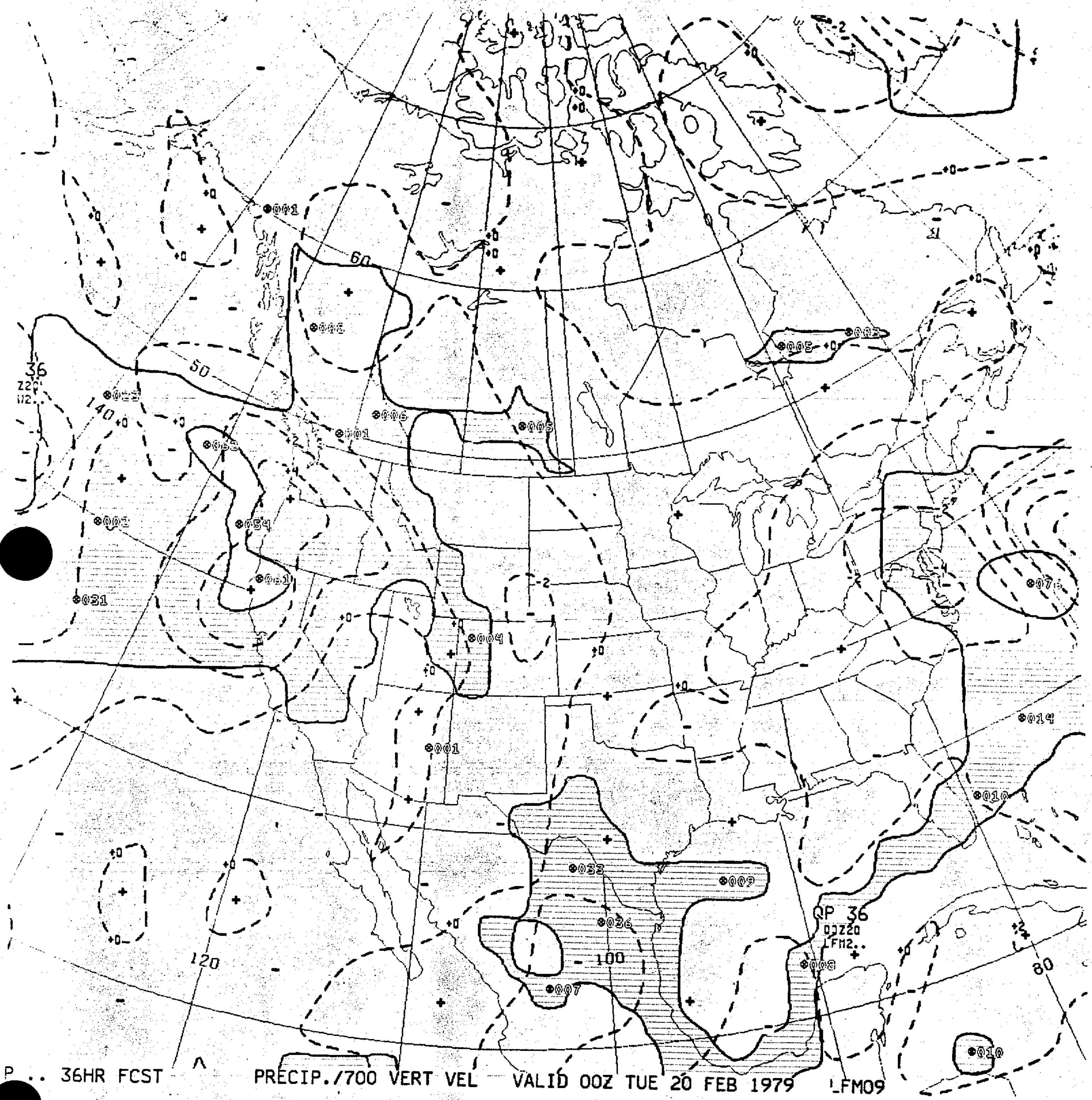
P .. 36HR FCST
PRECIP./700 VERT VEL
VALID 00Z TUE 20 FEB 1979
LFM09
QP 36
00Z20
LFM2..
60
50
140
120
100
80

FIGURE 10b

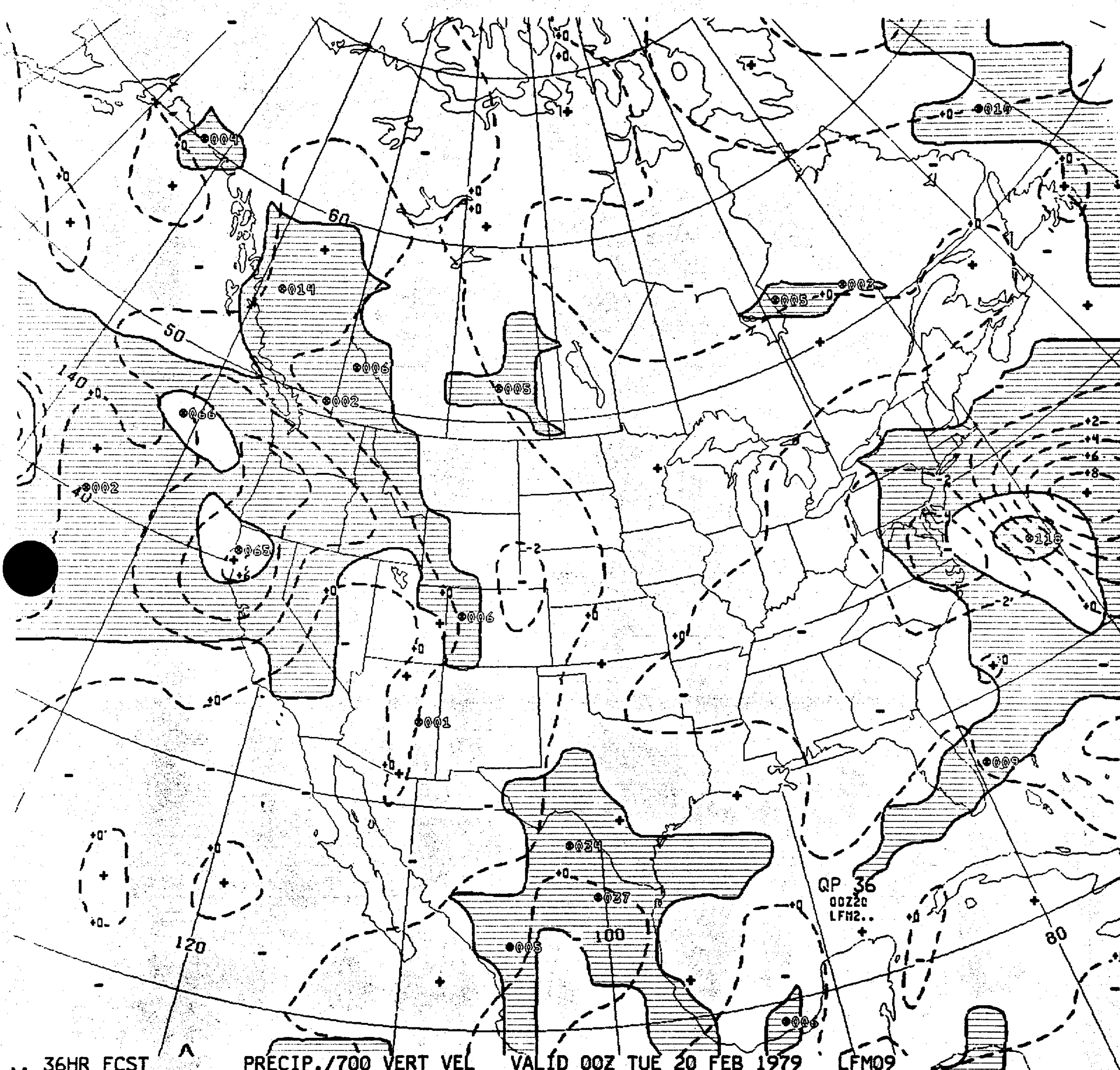

.. 36HR FCST PRECIP./700 VERT VEL VALID 00Z TUE 20 FEB 1979 LFM09
QP 36
00Z20
LFM2..

FIGURE 10c

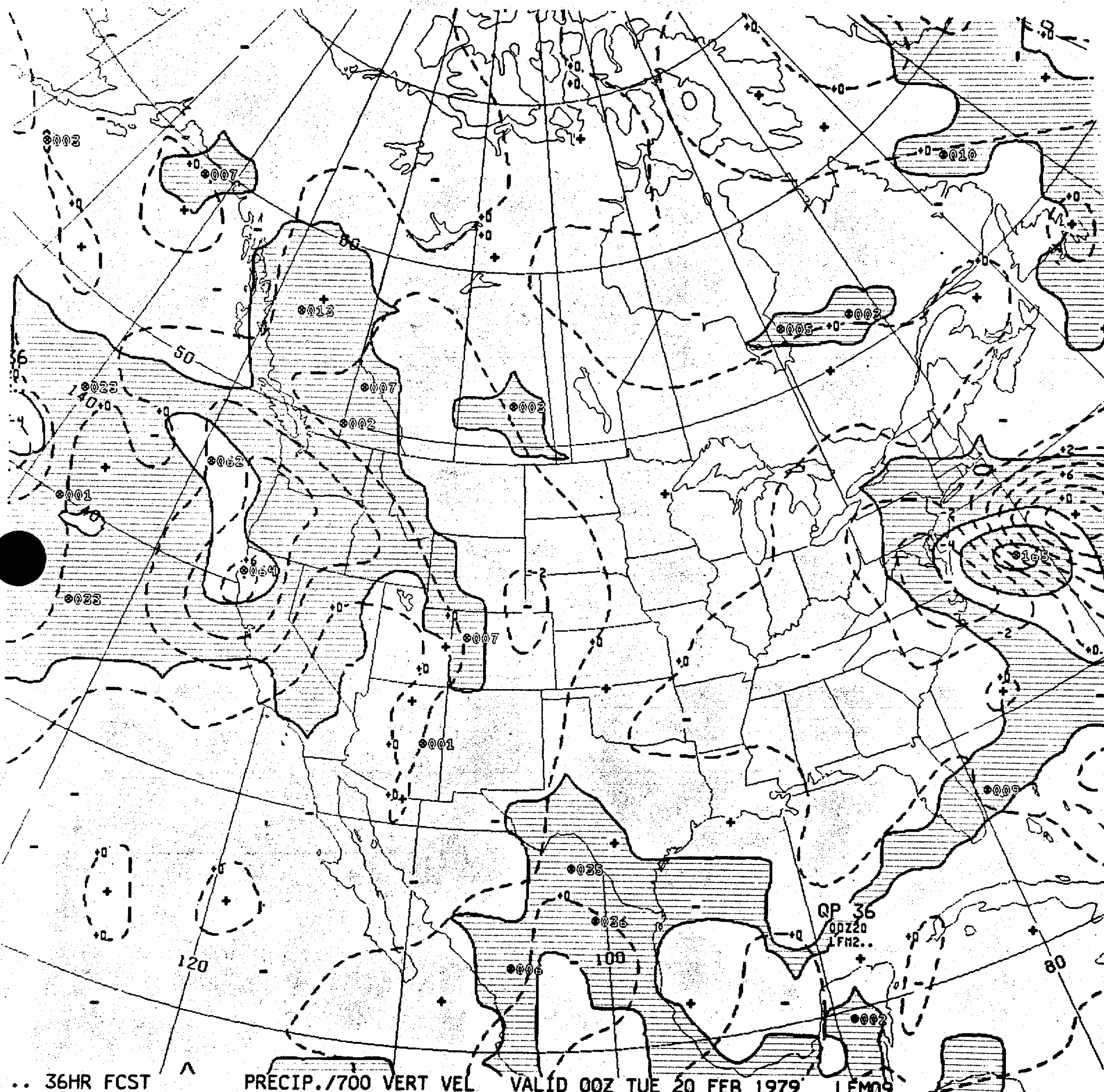
.. 36HR FCST PRECIP./700 VERT VEL VALID 00Z TUE 20 FEB 1979 LFM09
QP 36
00Z20
LFM2..
50
40
120
100
80

FIGURE 10d

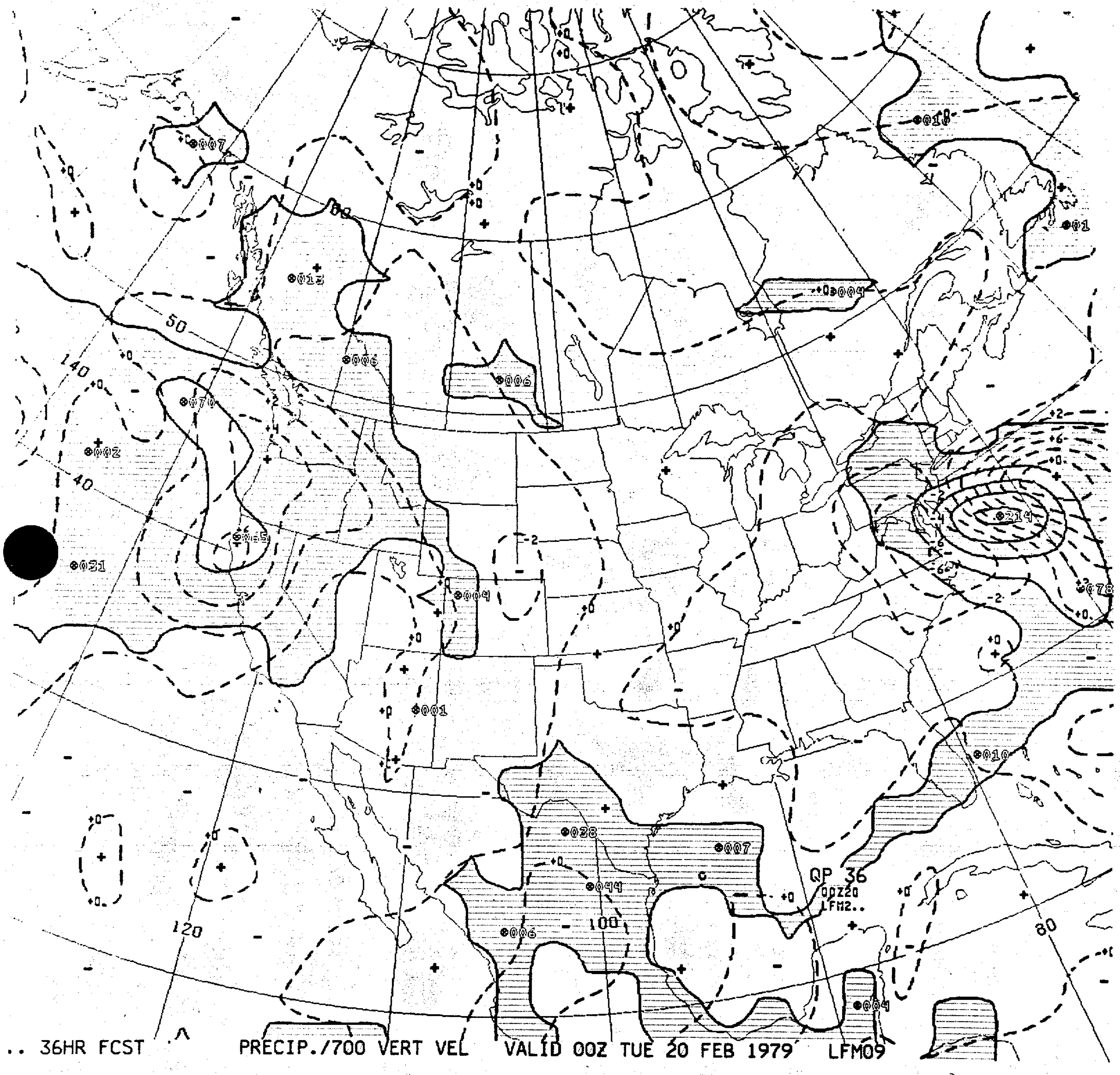
.. 36HR FCST
PRECIP./700 VERT VEL
VALID 00Z TUE 20 FEB 1979
LFM09
QP 36
00Z20
LFM2..

FIGURE 10e

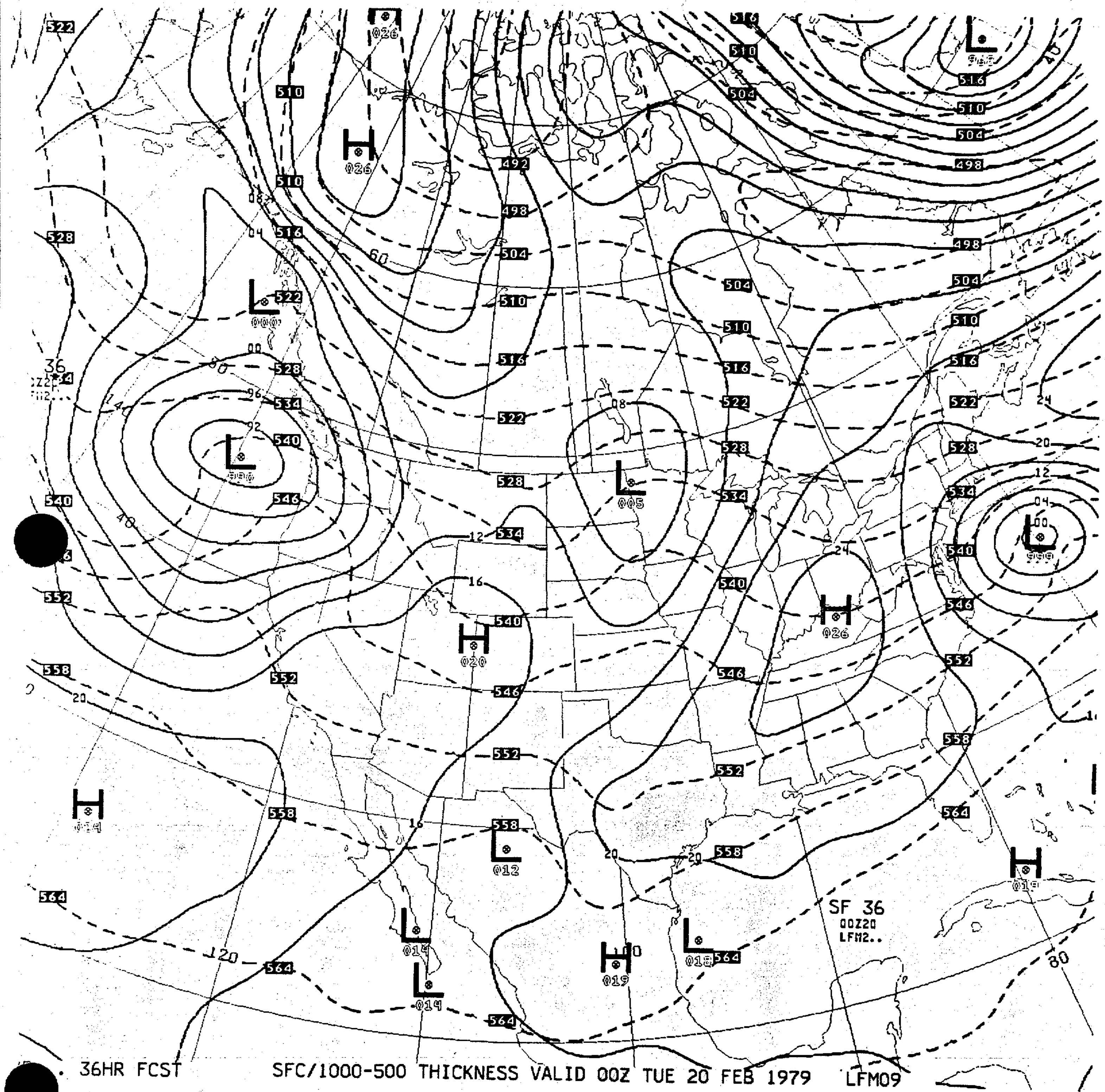
SF 36
00Z20
LFM2..
36HR FCST SFC/1000-500 THICKNESS VALID 00Z TUE 20 FEB 1979 LFM09

FIGURE 11a

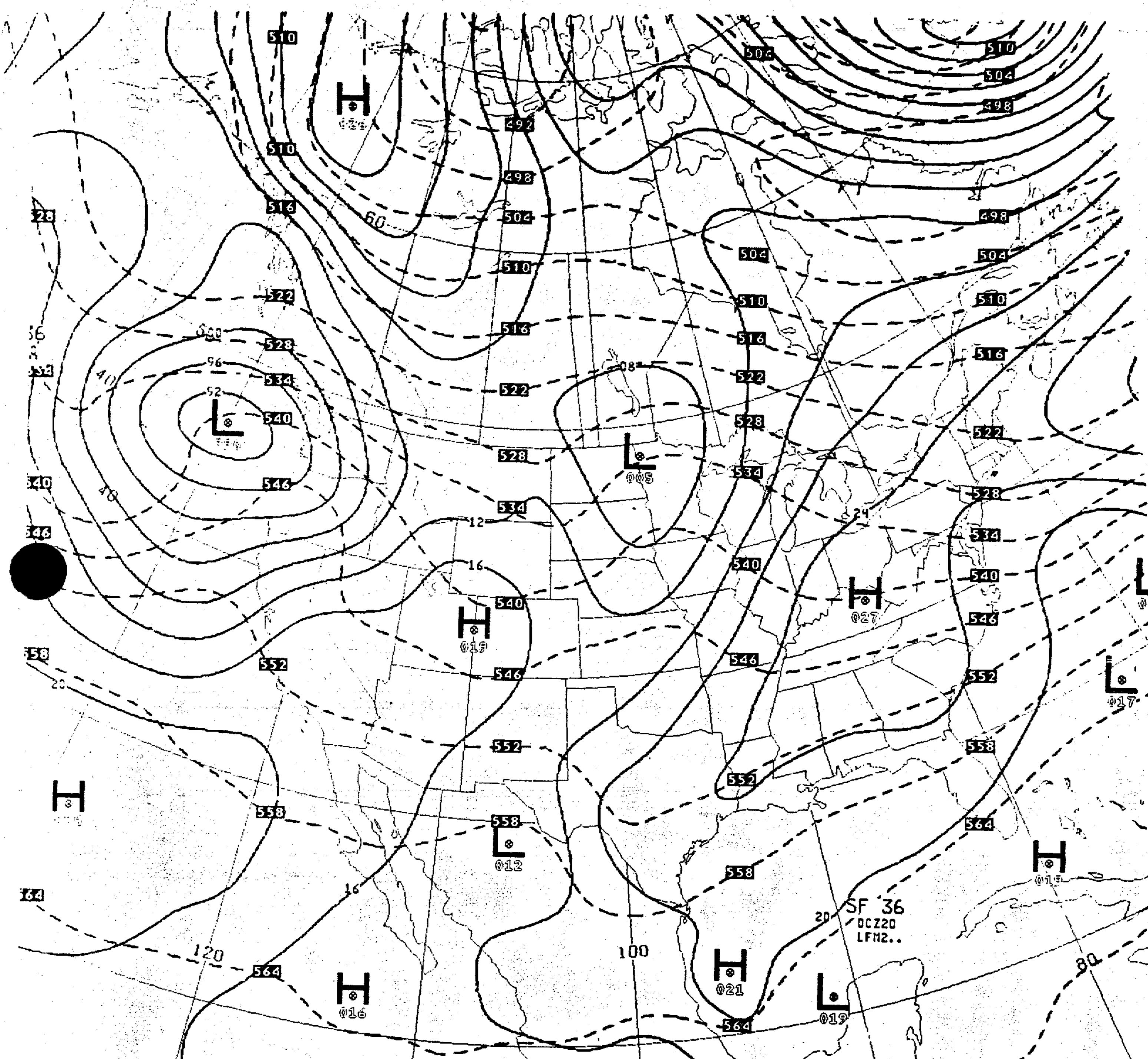

.. 36HR FCST SFC/1000-500 THICKNESS VALID 00Z TUE 20 FEB 1979 LFM09

FIGURE 11b

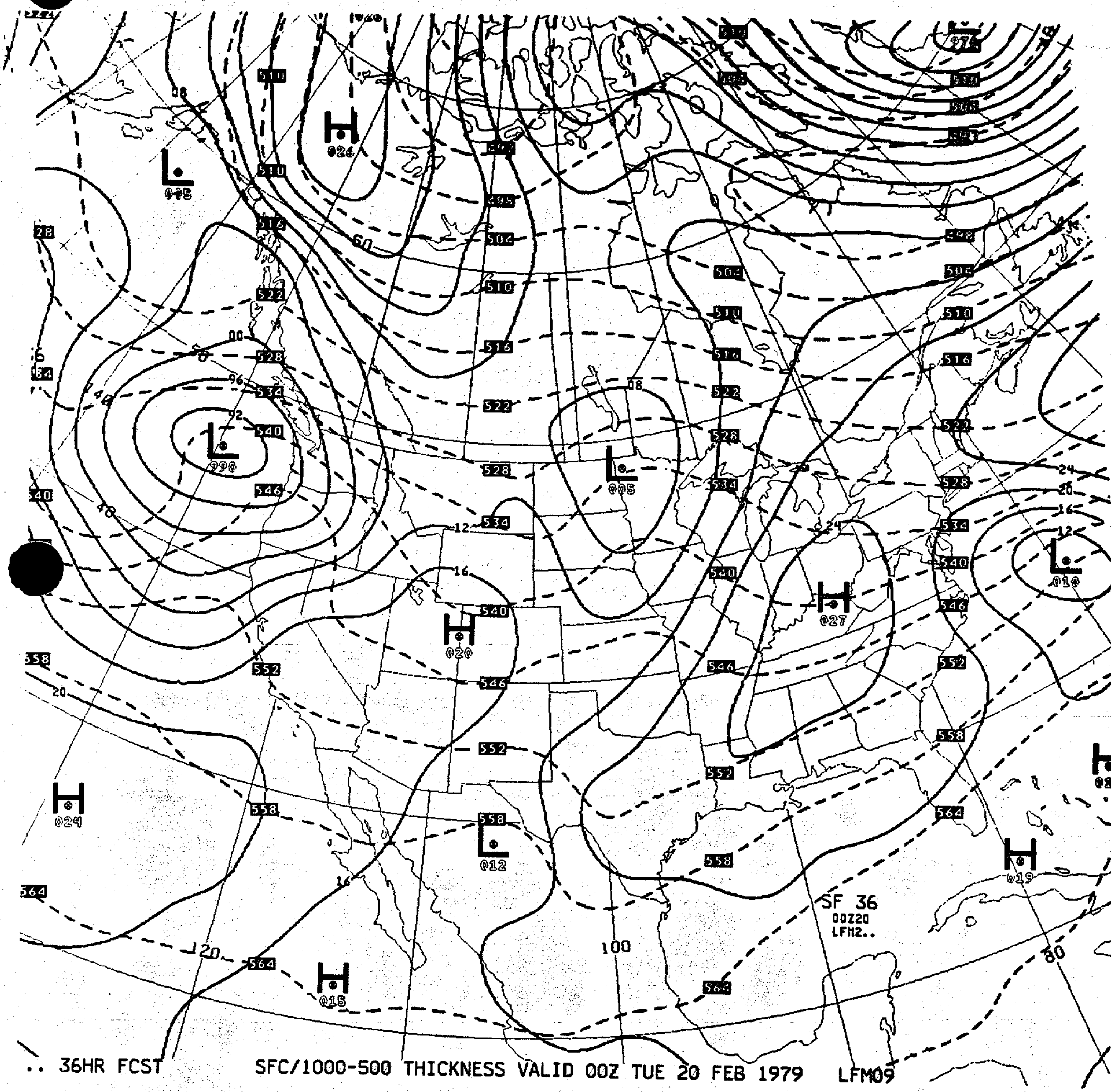
SF 36
00Z20
LFM2..
36HR FCST
SFC/1000-500 THICKNESS VALID 00Z TUE 20 FEB 1979
LFM09

FIGURE 11c

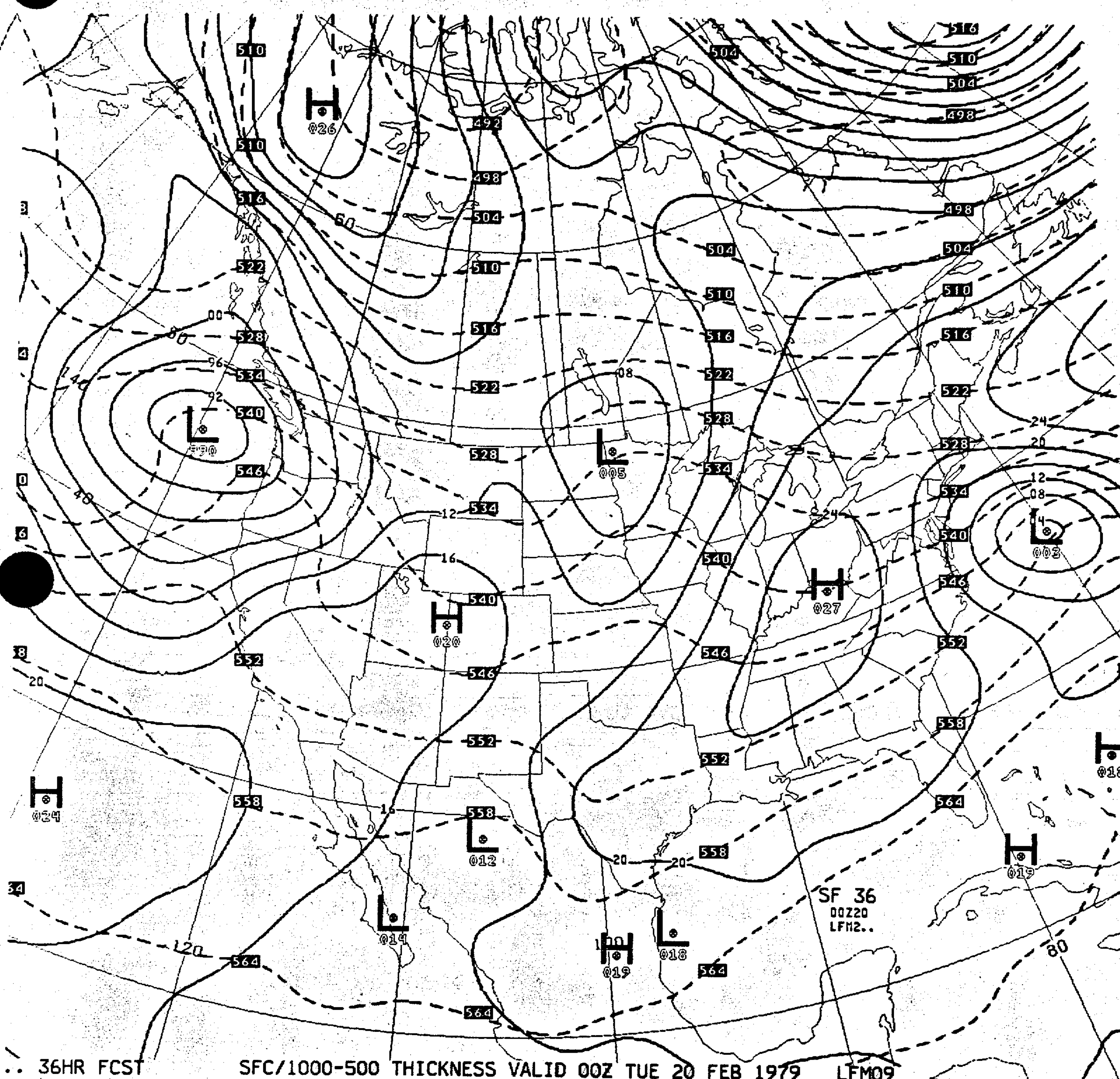

.. 36HR FCST SFC/1000-500 THICKNESS VALID 00Z TUE 20 FEB 1979 LFM09

FIGURE 11d

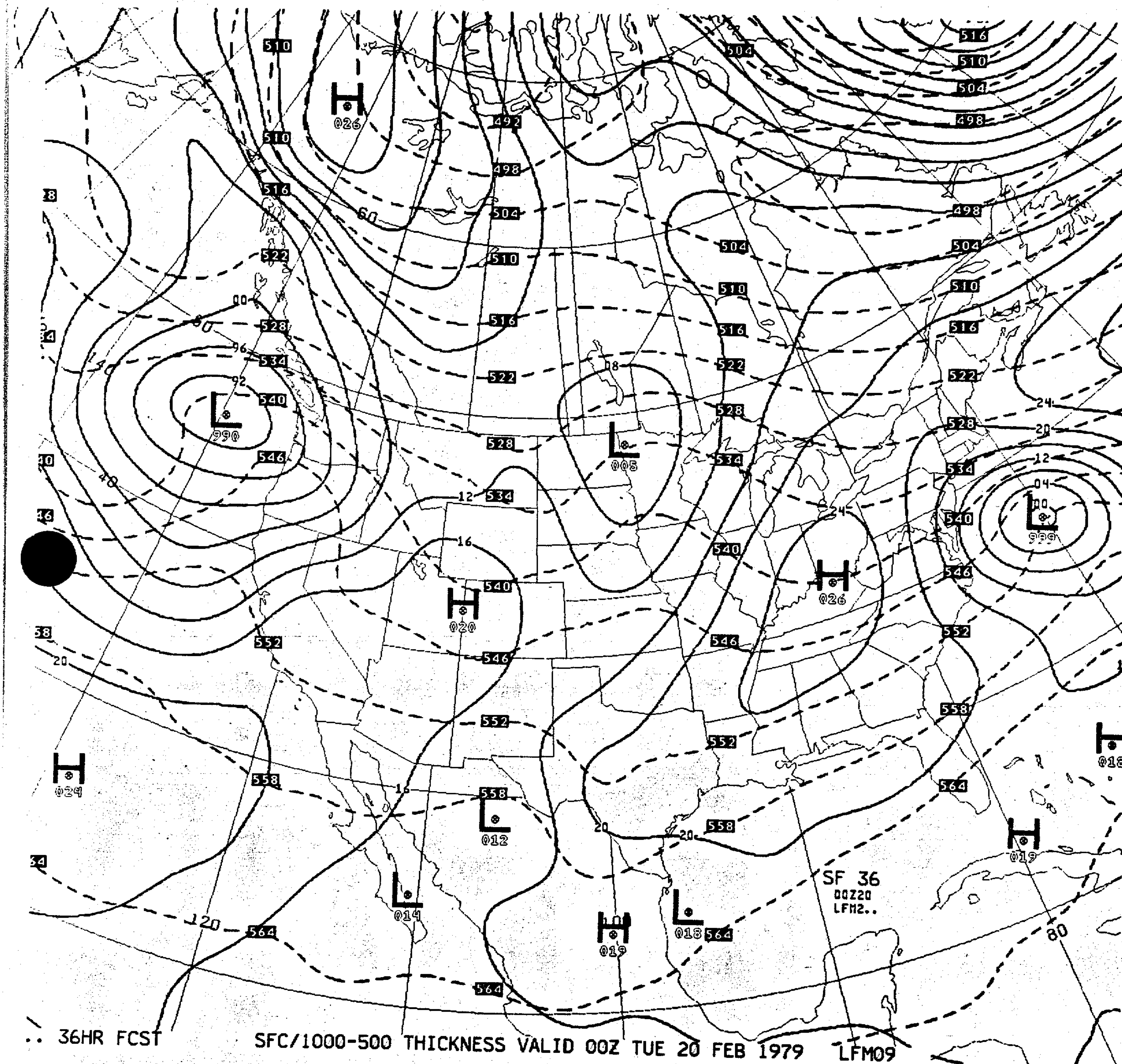
SF 36
00Z20
LFM2..
36HR FCST
SFC/1000-500 THICKNESS VALID 00Z TUE 20 FEB 1979
LFM09

FIGURE 11e